Blind Adaptive Space–Time Multiuser Detection With Multiple Transmitter and Receiver Antennas

Daryl Reynolds, Xiaodong Wang, *Member, IEEE*, and H. Vincent Poor, *Fellow, IEEE*

***Abstract*—The demand for performance and capacity in cellular systems has generated a great deal of interest in the development of advanced signal processing techniques to optimize the use of system resources. In particular, much recent work has been done on space–time processing in which multiple transmit/receive antennas are used in conjunction with coding to exploit spatial diversity. In this paper, we consider space–time multiuser detection using multiple transmit and receive antennas for code-division multiple-access (CDMA) communications. We compare, via analytical bit-error-probability calculations, user capacity, and complexity, two linear receiver structures for different antenna configurations. Motivated by its appearance in a number of third-genaeration (3G) wideband CDMA standards, we use the Alamouti space–time block code for two-transmit-antenna configurations. We also develop blind adaptive implementations for the two transmit/two receive antenna case for synchronous CDMA in flat-fading channels and for asynchronous CDMA in fading multipath channels. Finally, we present simulation results for the blind adaptive implementations.**

***Index Terms*—Blind adaptive receiver, multiple antennas, multiuser detection, space–time block code, subspace tracking, wireless communications.**

I. Introduction

THE EVER-increasing demand for performance and capacity in cellular wireless systems has prompted the development of myriad advanced signal processing techniques in an effort to utilize these resources more efficiently. The multiple-access technique that has received the most attention, and the one on which many of these signal processing techniques are based, is direct-sequence code-division multiple-access (DS-CDMA or, simply, CDMA). CDMA or wideband CDMA (WCDMA) is one of the more promising candidates for third-generation (3G) cellular services [1]. One of the new technologies that is being considered for 3G and later generation WCDMA standards is space–time processing. Generally speaking, space–time processing involves the exploitation of spatial diversity using multiple transmit and/or receive antennas and, perhaps, some form of coding. The initial focus was on systems that use one transmit antenna and multiple receive antennas [2]–[8]. Recently, however, much of the work in this area has focused on transmit diversity schemes that use multiple transmit antennas. They include delay schemes [9]–[12] in which copies of the same symbol are transmitted through multiple antennas at different times, the space–time trellis coding algorithm developed by Tarokh *et al.* in [13], and the simple space–time block coding (STBC) scheme developed by Alamouti [14], which has been adopted in a number of 3G WCDMA standards [15], [16]. A generalization of the Alamouti space–time block coding concept is developed in [17]. It has been shown that these techniques can significantly improve capacity [18], [19].

Recently, some work has been completed on space–time multiuser detection using multiple antennas at *both* the transmitter and receiver. In [20], for example, the authors considered maximum-likelihood space–time multiuser detection in a CDMA system using orthogonal spreading codes. An application of space–time block coding to CDMA appears in [21]. However, this work assumes a perfectly known channel and does not investigate blind adaptive algorithms or make use of the popular Alamouti space–time code. In the present work, we consider the performance of linear space–time multiuser detection using multiple transmit and receive antennas for CDMA systems using nonorthogonal codes. First, we will compare two different linear receiver structures (linear diversity combining and space–time detection) for various antenna configurations. Motivated by the use of STBC in 3G proposals, we will utilize this block code for two-transmit-antenna configurations. Then, we develop blind adaptive implementations of the two transmit/two receive antenna configuration for synchronous CDMA in flat-fading channels and for asynchronous CDMA in fading multipath channels. The adaptive techniques developed here are blind, in the sense that the only information known to the receiver is the signature sequence of the user of interest.

The remainder of this paper is organized as follows. In Section II, we analyze and compare two different linear receiver structures that are appropriate for CDMA with multiple transmit and/or receive antennas. In Section III, we develop blind adaptive implementations of the space–time receiver structure for synchronous CDMA in flat-fading channels. In Section IV, we extend the sequential adaptive implementation to asynchronous CDMA in fading multipath channels. In Section V, we present simulation results, and Section VI concludes the paper.

Manuscript received March 8, 2001; revised February 22, 2002. D. Reynolds and X. Wang were supported in part by the U.S. National Science Foundation (NSF) under Grants CCR-9875314 and CCR-9980599. H. V. Poor was supported in part by NSF Grant CCR-9980580 and the New Jersey Center for Wireless Telecommunications. The associate editor coordinating the review of this paper and approving it for publication was Dr. Alex C. Kot.

D. Reynolds is with the Department of Electrical Engineering, Texas A&M University, College Station, TX 77843 USA (e-mail: reynolds@ee.tamu.edu).

X. Wang was with the Department of Electrical Engineering, Texas A&M University, College Station, TX 77843 USA. He is now with the Department of Electrical Engineering, Columbia University, New York, NY 10027 USA (e-mail: wangx@ee.columbia.edu).

H. V. Poor is with the Department of Electrical Engineering, Princeton University, Princeton, NJ 08544 USA (e-mail: poor@ee.princeton.edu).

Publisher Item Identifier S 1053-587X(02)04388-X.

II. SPACE–TIME MULTIUSER DETECTION IN SYNCHRONOUS CDMA: ANALYSIS

In this section, we analyze receiver structures for synchronous CDMA systems with multiple transmitter antennas and multiple receiver antennas. Specifically, we focus on three configurations:

1) one transmitter antenna, two receiver antennas;
2) two transmitter antennas, one receiver antenna;
3) two transmitter antennas and two receiver antennas.

It is assumed that a space–time block code is employed in systems with two transmitter antennas. For each of these configurations, we discuss two possible linear receiver structures and compare their performance in terms of diversity gain and signal separation capability.

A. One Transmitter Antenna, Two Receiver Antennas

Consider the following discrete-time K-user synchronous CDMA channel with one transmitter antenna and two receiver antennas. The received baseband signal at the pth antenna can be modeled as

$$\boldsymbol{r}_p = \sum_{k=1}^{K} h_{p,k} b_k \boldsymbol{s}_k + \boldsymbol{n}_p, \qquad p = 1, 2 \tag{1}$$

where

$\boldsymbol{s}_k$	N vector of the discrete-time signature waveform of the kth user with unit norm, i.e., $\|\boldsymbol{s}_k\| = 1$;
$b_k \in \{+1, -1\}$	data bit of the kth user;
$h_{p,k}$	complex channel response of the pth receiver antenna element to the kth user's signal;
$\boldsymbol{n}_p \sim \mathcal{N}_c(\boldsymbol{0}, \sigma^2 \boldsymbol{I}_N)$	ambient noise vector at antenna p.

It is assumed that $\boldsymbol{n}_1$ and $\boldsymbol{n}_2$ are independent.

1) Linear Diversity Multiuser Detector: Denote

$$\boldsymbol{h}_k \triangleq [h_{1,k}\ h_{2,k}]^T$$
$$\boldsymbol{S} \triangleq [\boldsymbol{s}_1\ \cdots\ \boldsymbol{s}_K]$$
$$\boldsymbol{R} \triangleq \boldsymbol{S}^T \boldsymbol{S}.$$

Suppose that user 1 is the user of interest. We first consider the linear diversity multiuser detection scheme, which first applies a linear multiuser detector to the received signal $\boldsymbol{r}_p$ in (1) at each antenna $p = 1, 2$ and then combines the outputs of these linear detectors to make a decision. For example, a linear decorrelating detector for user 1 based on the signal in (1) is simply [22]

$$\boldsymbol{w}_1 = \boldsymbol{S}\boldsymbol{R}^{-1}\boldsymbol{e}_1 \tag{2}$$

where $\boldsymbol{e}_1$ denotes the first unit vector in $\mathbb{R}^K$. This detector is applied to the received signal at each antenna $p = 1, 2$ to obtain $\boldsymbol{z} = [z_1\ z_2]^T$, where

$$z_p \triangleq \boldsymbol{w}_1^T \boldsymbol{r}_p = h_{p,1} b_1 + u_p \tag{3}$$

with

$$u_p \triangleq \boldsymbol{w}_1^T \boldsymbol{n}_p \sim \mathcal{N}_c(\boldsymbol{0}, \sigma^2 \|\boldsymbol{w}_1\|^2), \qquad p = 1, 2 \tag{4}$$

where $\|\boldsymbol{w}_1\|^2 = [\boldsymbol{R}^{-1}]_{1,1}$ and where $[\boldsymbol{A}]_{i,j}$ denotes the element in the ith row and jth column of the matrix $\boldsymbol{A}$. Denote

$$\eta_1 \triangleq \frac{1}{\sqrt{[\boldsymbol{R}^{-1}]_{1,1}}}. \tag{5}$$

Denote $\boldsymbol{h}_k \triangleq [h_{1,k}\ \ h_{2,k}]^T$. Since the noise vectors from different antennas are independent, we can write

$$\boldsymbol{z} = b_1 \boldsymbol{h}_1 + \boldsymbol{u} \tag{6}$$

with

$$\boldsymbol{u} \sim \mathcal{N}_c\left(\boldsymbol{0}, \frac{\sigma^2}{\eta_1^2} \cdot \boldsymbol{I}_2\right). \tag{7}$$

The maximum likelihood (ML) decision rule for b_1 based on $\boldsymbol{z}$ in (6) is then

$$\hat{b}_1 = \text{sign}(\Re\{\boldsymbol{h}_1^H \boldsymbol{z}\}). \tag{8}$$

Let $E_1 \triangleq \boldsymbol{h}_1^H \boldsymbol{h}_1$ be the total received desired user's signal energy. The decision statistic in (8) can be expressed as

$$\xi \triangleq \boldsymbol{h}_1^H \boldsymbol{z} = E_1 b_1 + v \tag{9}$$

with

$$v \triangleq \boldsymbol{h}_1^H \boldsymbol{u} \sim \mathcal{N}_c(0, E_1 \sigma^2 / \eta_1^2). \tag{10}$$

The probability of detection error of the linear diversity multiuser detector is computed as

$$\begin{aligned} P_1^{\mathrm{D}}(e) &= P(\Re\{\xi\} < 0 \,|\, b_1 = 1) \\ &= P(\Re\{v\} < -E_1) = Q\left(\frac{\sqrt{2E_1}}{\sigma} \cdot \eta_1\right). \end{aligned} \tag{11}$$

2) Linear Space–Time Multiuser Detector: Denote

$$\boldsymbol{b} \triangleq [b_1 \cdots b_K]^T$$
$$\boldsymbol{H} \triangleq [\boldsymbol{h}_1 \cdots \boldsymbol{h}_K]$$
$$\tilde{\boldsymbol{s}}_k \triangleq \boldsymbol{h}_k \otimes \boldsymbol{s}_k$$
$$\tilde{\boldsymbol{S}} \triangleq [\tilde{\boldsymbol{s}}_1 \cdots \tilde{\boldsymbol{s}}_K]$$
$$\tilde{\boldsymbol{R}} \triangleq \tilde{\boldsymbol{S}}^H \tilde{\boldsymbol{S}}$$
$$\tilde{\boldsymbol{r}} \triangleq [\boldsymbol{r}_1^T\ \boldsymbol{r}_2^T]^T$$
$$\tilde{\boldsymbol{n}} \triangleq [\boldsymbol{n}_1^T\ \boldsymbol{n}_2^T]^T$$

where $\otimes$ denotes the Kronecker product. Then, by augmenting the received signals at two antennas, (1) can be written as

$$\tilde{\boldsymbol{r}} = \sum_{k=1}^{K} b_k \tilde{\boldsymbol{s}}_k + \tilde{\boldsymbol{n}} = \tilde{\boldsymbol{S}}\boldsymbol{b} + \tilde{\boldsymbol{n}} \tag{12}$$

with $\tilde{\boldsymbol{n}} \sim \mathcal{N}_c(\boldsymbol{0}, \sigma^2 \boldsymbol{I}_{2N})$. A linear space–time multiuser detector operates on the augmented received signal $\tilde{\boldsymbol{r}}$ directly. For example, the linear decorrelating detector for user 1 in this case is given by

$$\tilde{\boldsymbol{w}}_1 = \tilde{\boldsymbol{S}}\tilde{\boldsymbol{R}}^{-1}\boldsymbol{e}_1. \tag{13}$$

This detector is applied to the augmented received signal $\tilde{\boldsymbol{r}}$ to obtain

$$\tilde{z} \triangleq \tilde{\boldsymbol{w}}_1^H \tilde{\boldsymbol{r}} = b_1 + \tilde{u} \tag{14}$$

with

$$\tilde{u} \triangleq \tilde{\boldsymbol{w}}_1^H \tilde{\boldsymbol{n}} \sim \mathcal{N}_c(\boldsymbol{0}, \sigma^2 \|\tilde{\boldsymbol{w}}_1\|^2) \tag{15}$$

where $\|\tilde{\boldsymbol{w}}_1\|^2 = [\tilde{\boldsymbol{R}}^{-1}]_{1,1}$. Denote

$$\tilde{\eta}_1 \triangleq \frac{1}{\sqrt{E_1}} \cdot \frac{1}{\sqrt{\left[\tilde{\boldsymbol{R}}^{-1}\right]_{1,1}}}. \tag{16}$$

An expression for $\tilde{\boldsymbol{R}}$ can be found as follows. Note that

$$\begin{aligned}\left[\tilde{\boldsymbol{R}}\right]_{i,j} &\triangleq \left[\tilde{\boldsymbol{S}}^H\tilde{\boldsymbol{S}}\right]_{i,j} = \tilde{\boldsymbol{s}}_i^H\tilde{\boldsymbol{s}}_j \\ &= (\boldsymbol{h}_i \otimes \boldsymbol{s}_i)^H(\boldsymbol{h}_j \otimes \boldsymbol{s}_j) = (\boldsymbol{h}_i^H \otimes \boldsymbol{s}_i^T)(\boldsymbol{h}_j \otimes \boldsymbol{s}_j) \\ &= (\boldsymbol{h}_i^H\boldsymbol{h}_j) \otimes (\boldsymbol{s}_i^T\boldsymbol{s}_j) = [\boldsymbol{H}^H\boldsymbol{H}]_{i,j} \cdot [\boldsymbol{R}]_{i,j}.\end{aligned} \tag{17}$$

Hence

$$\tilde{\boldsymbol{R}} \triangleq \tilde{\boldsymbol{S}}^H\tilde{\boldsymbol{S}} = \boldsymbol{R} \circ (\boldsymbol{H}^H\boldsymbol{H}) \tag{18}$$

where $\circ$ denotes the Schur matrix product (i.e., element-wise product).

The ML decision rule for b_1 based on $\tilde{z}$ in (14) is then

$$\hat{b}_1 = \text{sign}(\Re\{\tilde{z}\}). \tag{19}$$

The probability of detection error of the space time multiuser detector is computed as

$$\begin{aligned}P_1^{\text{ST}}(e) &= P(\Re\{\tilde{z}\} < 0 \,|\, b_1 = 1) \\ &= P(\Re\{\tilde{u}\} < -1) = Q\left(\frac{\sqrt{2E_1}}{\sigma} \cdot \tilde{\eta}_1\right).\end{aligned} \tag{20}$$

3) Performance Comparison: From the above discussion, it is seen that the linear space–time multiuser detector exploits the signal structure in both the time domain (i.e., induced by the signature waveform $\boldsymbol{s}_k$) and the spatial domain (i.e., induced by the channel response $\boldsymbol{h}_k$) for interference rejection, whereas for the linear diversity multiuser detector, interference rejection is performed only in the time domain, and the spatial domain is only used for diversity combining. The next result, which first appeared in [7], shows that the linear space–time multiuser detector always outperforms the linear diversity multiuser detector.

Proposition 1: Let $P_1^{\text{D}}(e)$ given by (11) and $P_k^{\text{ST}}(e)$ given by (20) be, respectively, the probability of detection error of the linear diversity detector and the linear space–time detector. Then

$$P_1^{\text{ST}}(e) \le P_1^{\text{D}}(e).$$

B. Two Transmitter Antennas, One Receiver Antenna

When two antennas are employed at the transmitter, we must first specify how the information bits are transmitted across the two antennas. Here, we adopt the Alamouti space–time block coding scheme [14], [17]. Specifically, for each user k, two information symbols $b_{1,k}$ and $b_{2,k}$ are transmitted over two symbol intervals. At the first time interval, the symbol pair $(b_{1,k}, b_{2,k})$ is transmitted across the two transmitter antennas, and at the second time interval, the symbol pair $(-b_{2,k}, b_{1,k})$ is transmitted. The received signal corresponding to these two time intervals are given by

$$\boldsymbol{r}_1 = \sum_{k=1}^{K}(h_{1,k}b_{1,k} + h_{2,k}b_{2,k})\boldsymbol{s}_k + \boldsymbol{n}_1 \tag{21}$$

$$\boldsymbol{r}_2 = \sum_{k=1}^{K}(-h_{1,k}b_{2,k} + h_{2,k}b_{1,k})\boldsymbol{s}_k + \boldsymbol{n}_2 \tag{22}$$

where $h_{1,k}$ ($h_{2,k}$) is the complex channel responses between the first (second) transmitter antenna and the receiver antenna, and $\boldsymbol{n}_1$ and $\boldsymbol{n}_2$ are independent received $\mathcal{N}_c(\boldsymbol{0}, \boldsymbol{I}_N)$ noise vectors at the two time intervals.

1) Linear Diversity Multiuser Detector: We first consider the linear diversity multiuser detection scheme, which first applies the linear multiuser detector $\boldsymbol{w}_1$ in (2) to the received signals $\boldsymbol{r}_1$ and $\boldsymbol{r}_2$ during the two time intervals, and then performs a space–time decoding. Specifically, denote

$$z_1 \triangleq \boldsymbol{w}_1^T\boldsymbol{r}_1 = h_{1,k}b_{1,k} + h_{2,k}b_{2,k} + u_1 \tag{23}$$

$$z_2 \triangleq (\boldsymbol{w}_1^T\boldsymbol{r}_2)^* = -h_{1,k}^*b_{2,k} + h_{2,k}^*b_{1,k} + u_2^* \tag{24}$$

with

$$u_p \triangleq \boldsymbol{w}_1^T\boldsymbol{n}_p \sim \mathcal{N}_c(\boldsymbol{0}, \sigma^2\|\boldsymbol{w}_1\|^2), \qquad p = 1, 2 \tag{25}$$

where $\|\boldsymbol{w}_1\|^2 = [\boldsymbol{R}^{-1}]_{1,1}$.

Denote

$$\boldsymbol{z} \triangleq \begin{bmatrix} z_1 \\ z_2 \end{bmatrix}, \qquad \boldsymbol{u} \triangleq \begin{bmatrix} u_1 \\ u_2^* \end{bmatrix}$$

$$\boldsymbol{h}_k \triangleq \begin{bmatrix} h_{1,k} \\ h_{2,k}^* \end{bmatrix}, \qquad \overline{\boldsymbol{h}}_k \triangleq \begin{bmatrix} h_{2,k} \\ -h_{1,k}^* \end{bmatrix}.$$

It is easily seen that $\boldsymbol{h}_k^H\overline{\boldsymbol{h}}_k = 0$. Then, (23)–(25) can be written as

$$\boldsymbol{z} = \left[\boldsymbol{h}_1 \; \overline{\boldsymbol{h}}_1\right]\begin{bmatrix} b_{1,1} \\ b_{2,1} \end{bmatrix} + \boldsymbol{u} \tag{26}$$

with

$$\boldsymbol{u} \sim \mathcal{N}_c\left(\boldsymbol{0}, \frac{\sigma^2}{\eta_1^2} \cdot \boldsymbol{I}_2\right). \tag{27}$$

As before, denote $E_1 \triangleq \boldsymbol{h}_1^H\boldsymbol{h}_1 = \overline{\boldsymbol{h}}_1^H\overline{\boldsymbol{h}}_1$. Note that

$$\left[\boldsymbol{h}_1 \; \overline{\boldsymbol{h}}_1\right]^H\left[\boldsymbol{h}_1 \; \overline{\boldsymbol{h}}_1\right] = \begin{bmatrix} E_1 & 0 \\ 0 & E_1 \end{bmatrix}. \tag{28}$$

The ML decision rule for $b_{1,1}$ and $b_{2,1}$ based on $\boldsymbol{z}$ in (26) is then given by

$$\begin{aligned}\begin{bmatrix} \hat{b}_{1,1} \\ \hat{b}_{2,1} \end{bmatrix} &= \text{sign}\left(\Re\left\{\left[\boldsymbol{h}_1 \; \overline{\boldsymbol{h}}_1\right]^H\boldsymbol{z}\right\}\right) \\ &= \text{sign}\left(\Re\left\{\begin{bmatrix} \boldsymbol{h}_1^H\boldsymbol{z} \\ \overline{\boldsymbol{h}}_1^H\boldsymbol{z} \end{bmatrix}\right\}\right).\end{aligned} \tag{29}$$

Using (26), it is easily seen that the decision statistic in (29) is distributed according to

$$\frac{1}{\sqrt{E_1}}\boldsymbol{h}_1^H\boldsymbol{z} \sim \mathcal{N}_c\left(\sqrt{E_1}b_{1,1}, \frac{\sigma^2}{\eta_1^2}\right) \tag{30}$$

$$\frac{1}{\sqrt{E_1}}\overline{\boldsymbol{h}}_1^H\boldsymbol{z} \sim \mathcal{N}_c\left(\sqrt{E_1}b_{2,1}, \frac{\sigma^2}{\eta_1^2}\right). \tag{31}$$

Hence, the probability of error is given by

$$P_1^{\text{D}}(e) = Q\left(\frac{\sqrt{2E_1}}{\sigma} \cdot \eta_1\right). \tag{32}$$

This is the same expression as (20) for the linear diversity receiver with one transmitter antenna and two receiver antennas.

2) Linear Space–Time Multiuser Detector: Denote

$$\tilde{\boldsymbol{r}} \triangleq \begin{bmatrix} \boldsymbol{r}_1 \\ \boldsymbol{r}_2^* \end{bmatrix}, \qquad \tilde{\boldsymbol{n}} \triangleq \begin{bmatrix} \boldsymbol{n}_1 \\ \boldsymbol{n}_2^* \end{bmatrix}.$$

Then, (21) and (22) can be written as

$$\tilde{\boldsymbol{r}} = \sum_{k=1}^{K} \left(b_{1,k} \boldsymbol{h}_k \otimes \boldsymbol{s}_k + b_{2,k} \overline{\boldsymbol{h}}_k \otimes \boldsymbol{s}_k \right) + \tilde{\boldsymbol{n}}. \tag{33}$$

Denote

$$\tilde{\boldsymbol{S}} = \left[\boldsymbol{h}_1 \otimes \boldsymbol{s}_1,\, \overline{\boldsymbol{h}}_1 \otimes \boldsymbol{s}_1,\, \ldots,\, \boldsymbol{h}_K \otimes \boldsymbol{s}_K,\, \overline{\boldsymbol{h}}_K \otimes \boldsymbol{s}_K \right]_{2N \times 2K} \tag{34}$$

$$\tilde{\boldsymbol{R}} = \tilde{\boldsymbol{S}}^H \tilde{\boldsymbol{S}}. \tag{35}$$

Then, the decorrelating detector for detecting the bit $b_{1,1}$ based on $\tilde{\boldsymbol{r}}$ in (33) is given by

$$\tilde{\boldsymbol{w}}_{1,1} = \tilde{\boldsymbol{S}} \tilde{\boldsymbol{R}}^{-1} \tilde{\boldsymbol{e}}_1 \tag{36}$$

where $\tilde{\boldsymbol{e}}_1$ is the first unit vector in $\mathbb{R}^{2K}$.

Proposition 2: The decorrelating detector in (36) is given by

$$\tilde{\boldsymbol{w}}_{1,1} = \frac{\boldsymbol{h}_1 \otimes \boldsymbol{w}_1}{\|\boldsymbol{h}_1\|^2} \tag{37}$$

where $\boldsymbol{w}_1$ is given by (2).

Proof: We need to verify that

$$\left(\frac{\boldsymbol{h}_1 \otimes \boldsymbol{w}_1}{\|\boldsymbol{h}_1\|^2} \right)^H \tilde{\boldsymbol{S}} = \tilde{\boldsymbol{e}}_1. \tag{38}$$

We have

$$\begin{aligned} &\frac{1}{\|\boldsymbol{h}_1\|^2} (\boldsymbol{h}_1 \otimes \boldsymbol{w}_1)^H (\boldsymbol{h}_1 \otimes \boldsymbol{s}_1) \\ &\quad = \frac{1}{\|\boldsymbol{h}_1\|^2} (\boldsymbol{h}_1^H \boldsymbol{h}_1) \underbrace{(\boldsymbol{w}_1^T \boldsymbol{s}_1)}_{1} = 1 \end{aligned} \tag{39}$$

$$\begin{aligned} &\frac{1}{\|\boldsymbol{h}_1\|^2} (\boldsymbol{h}_1 \otimes \boldsymbol{w}_1)^H \left(\overline{\boldsymbol{h}}_1 \otimes \boldsymbol{s}_1 \right) \\ &\quad = \frac{1}{\|\boldsymbol{h}_1\|^2} \frac{1}{\|\boldsymbol{h}_1\|^2} \underbrace{\left(\boldsymbol{h}_1^H \overline{\boldsymbol{h}}_1 \right)}_{0} \underbrace{(\boldsymbol{w}_1^T \boldsymbol{s}_1)}_{1} = 0 \end{aligned} \tag{40}$$

$$\begin{aligned} &\frac{1}{\|\boldsymbol{h}_1\|^2} (\boldsymbol{h}_1 \otimes \boldsymbol{w}_1)^H (\boldsymbol{h}_k \otimes \boldsymbol{s}_k) \\ &\quad = \frac{1}{\|\boldsymbol{h}_1\|^2} (\boldsymbol{h}_1^H \boldsymbol{h}_k) \underbrace{(\boldsymbol{w}_1^T \boldsymbol{s}_k)}_{0} = 0, \qquad k = 2, \ldots, K \end{aligned} \tag{41}$$

$$\begin{aligned} &\frac{1}{\|\boldsymbol{h}_1\|^2} (\boldsymbol{h}_1 \otimes \boldsymbol{w}_1)^H \left(\overline{\boldsymbol{h}}_k \otimes \boldsymbol{s}_k \right) \\ &\quad = \frac{1}{\|\boldsymbol{h}_1\|^2} \left(\boldsymbol{h}_1^H \overline{\boldsymbol{h}}_k \right) \underbrace{(\boldsymbol{w}_1^T \boldsymbol{s}_k)}_{0} = 0, \qquad k = 2, \ldots, K. \end{aligned} \tag{42}$$

This verifies (38) so that (37) is indeed the decorrelating detector given by (36). □

Hence, the output of the linear space–time detector in this case is given by

$$\tilde{z}_1 = \tilde{\boldsymbol{w}}_{1,1}^H \tilde{\boldsymbol{r}} = b_{1,1} + u_1 \tag{43}$$

with

$$u_1 \triangleq \tilde{\boldsymbol{w}}_{1,1}^H \tilde{\boldsymbol{n}} \sim \mathcal{N}_c(0,\, \sigma^2 \|\tilde{\boldsymbol{w}}_{1,1}\|^2) \tag{44}$$

where, by using (5) and (37), we have

$$\|\tilde{\boldsymbol{w}}_{1,1}\|^2 = \frac{\|\boldsymbol{h}_1 \otimes \boldsymbol{w}_1\|^2}{\|\boldsymbol{h}_1\|^4} = \frac{\|\boldsymbol{w}_1\|^2}{\|\boldsymbol{h}_1\|^2} = \frac{1}{E_1 \eta_1^2}. \tag{45}$$

Therefore, the probability of detection error is given by

$$\begin{aligned} P_1^{\mathrm{ST}}(e) &= P(\Re\{\tilde{z}_1\} < 0 \,|\, b_{1,1} = 1) \\ &= P(\Re\{u_1\} < -1) = Q\left(\frac{\sqrt{2E_1}}{\sigma} \cdot \eta_1 \right). \end{aligned} \tag{46}$$

Comparing (32) with (46), we see that for the case of two transmitter antennas and one receiver antenna, the linear diversity receiver and the linear space–time receiver have the same performance. Hence, multiple transmitter antennas with space–time block coding only provide diversity gain but no signal separation capability.

C. Two Transmitter and Two Receiver Antennas

We combine the results from the previous two sections to investigate an environment in which we use two transmitter antennas and two receiver antennas. We adopt the space–time block coding scheme used in the previous section. The received signal at antenna 1 during the two symbol intervals is

$$\boldsymbol{r}_1^{(1)} = \sum_{k=1}^{K} \left[h_k^{(1,1)} b_{1,k} + h_k^{(2,1)} b_{2,k} \right] \boldsymbol{s}_k + \boldsymbol{n}_1^{(1)} \tag{47}$$

$$\boldsymbol{r}_2^{(1)} = \sum_{k=1}^{K} \left[-h_k^{(1,1)} b_{2,k} + h_k^{(2,1)} b_{1,k} \right] \boldsymbol{s}_k + \boldsymbol{n}_2^{(1)} \tag{48}$$

and the corresponding signals received at antenna 2 are

$$\boldsymbol{r}_1^{(2)} = \sum_{k=1}^{K} \left[h_k^{(1,2)} b_{1,k} + h_k^{(2,2)} b_{2,k} \right] \boldsymbol{s}_k + \boldsymbol{n}_1^{(2)} \tag{49}$$

$$\boldsymbol{r}_2^{(2)} = \sum_{k=1}^{K} \left[-h_k^{(1,2)} b_{2,k} + h_k^{(2,2)} b_{1,k} \right] \boldsymbol{s}_k + \boldsymbol{n}_2^{(2)} \tag{50}$$

where $h_k^{(i,j)}$, $i, j \in \{1, 2\}$ is the complex channel response between transmitter antenna i and receiver antenna j for user k. The noise vectors $\boldsymbol{n}_1^{(1)}$, $\boldsymbol{n}_1^{(2)}$, $\boldsymbol{n}_2^{(1)}$, and $\boldsymbol{n}_2^{(2)}$ are independent and identically distributed with distribution $\mathcal{N}_c(\boldsymbol{0},\, \sigma^2 \boldsymbol{I}_N)$.

1) Linear Diversity Multiuser Detector: As before, we first consider the linear diversity multiuser detection scheme for user 1, which applies the linear multiuser detector $\boldsymbol{w}_1$ in (2) to each of the four received signals $\boldsymbol{r}_1^{(1)}$, $\boldsymbol{r}_1^{(2)}$, $\boldsymbol{r}_2^{(1)}$, and $\boldsymbol{r}_2^{(2)}$ and then performs a space–time decoding. Specifically, denote the filter outputs as

$$z_1^{(1)} \triangleq \boldsymbol{w}_1^T \boldsymbol{r}_1^{(1)} = h_1^{(1,1)} b_{1,1} + h_1^{(2,1)} b_{2,1} + u_1^{(1)} \tag{51}$$

$$\begin{aligned} z_2^{(1)} &\triangleq \left(\boldsymbol{w}_1^T \boldsymbol{r}_2^{(1)} \right)^* = -\left(h_1^{(1,1)} \right)^* b_{2,1} \\ &\quad + \left(h_1^{(2,1)} \right)^* b_{1,1} + \left(u_2^{(1)} \right)^* \end{aligned} \tag{52}$$

$$z_1^{(2)} \triangleq \boldsymbol{w}_1^T \boldsymbol{r}_1^{(2)} = h_1^{(1,2)} b_{1,1} + h_1^{(2,2)}\; b_{2,1} + u_1^{(2)} \tag{53}$$

$$\begin{aligned} z_2^{(2)} &\triangleq \left(\boldsymbol{w}_1^T \boldsymbol{r}_2^{(2)} \right)^* = -\left(h_1^{(1,2)} \right)^* b_{2,1} \\ &\quad + \left(h_1^{(2,2)} \right)^* b_{1,1} + \left(u_2^{(2)} \right)^* \end{aligned} \tag{54}$$

with

$$u_i^{(j)} \triangleq \boldsymbol{w}_1^T \boldsymbol{n}_i^{(j)} \sim \mathcal{N}_c\left(\boldsymbol{0},\, \frac{\sigma^2}{\eta_1^2}\right), \qquad i, j = 1, 2 \tag{55}$$

where, as before, $\eta_1^2 \triangleq 1/[\boldsymbol{R}^{-1}]_{1,1}$.

We define the following quantities:

$$\begin{aligned}
\boldsymbol{z} &\triangleq [z_1^{(1)}\ z_2^{(1)}\ z_1^{(2)}\ z_2^{(2)}]^T \\
\boldsymbol{u} &\triangleq \left[u_1^{(1)}\ \left(u_2^{(1)}\right)^*\ u_1^{(2)}\ \left(u_2^{(2)}\right)^*\right]^T \\
\boldsymbol{h}_1^{(1)} &\triangleq \left[h_1^{(1,1)}\ h_1^{(2,1)}\right]^H \\
\overline{\boldsymbol{h}}_1^{(1)} &\triangleq \left[h_1^{(2,1)}\ -h_1^{(1,1)}\right]^T \\
\boldsymbol{h}_1^{(2)} &\triangleq \left[h_1^{(1,2)}\ h_1^{(2,2)}\right]^H \\
\overline{\boldsymbol{h}}_1^{(2)} &\triangleq \left[h_1^{(2,2)}\ -h_1^{(1,2)}\right]^T.
\end{aligned}$$

Then, (51)–(55) can be written as

$$\boldsymbol{z} = \underbrace{\left[\boldsymbol{h}_1^{(1)}\ \overline{\boldsymbol{h}}_1^{(1)}\ \boldsymbol{h}_1^{(2)}\ \overline{\boldsymbol{h}}_1^{(2)}\right]^H}_{\boldsymbol{H}_1^H} \begin{bmatrix} b_{1,1} \\ b_{2,1} \end{bmatrix} + \boldsymbol{u} \tag{56}$$

with

$$\boldsymbol{u} \sim \mathcal{N}_c\left(\boldsymbol{0},\, \frac{\sigma^2}{\eta_1^2} \cdot \boldsymbol{I}_4\right). \tag{57}$$

It is readily verified that

$$\boldsymbol{H}_1 \boldsymbol{H}_1^H = \begin{bmatrix} E_1 & 0 \\ 0 & E_1 \end{bmatrix} \tag{58}$$

with

$$E_1 \triangleq \left|h_1^{(1,1)}\right|^2 + \left|h_1^{(1,2)}\right|^2 + \left|h_1^{(2,1)}\right|^2 + \left|h_1^{(2,2)}\right|^2. \tag{59}$$

To form the ML decision statistic, we premultiply $\boldsymbol{z}$ by $\boldsymbol{H}_1$ and obtain

$$\begin{bmatrix} d_{1,1} \\ d_{2,1} \end{bmatrix} \triangleq \boldsymbol{H}_1 \boldsymbol{z} = E_1 \begin{bmatrix} b_{1,1} \\ b_{2,1} \end{bmatrix} + \boldsymbol{v} \tag{60}$$

with

$$\boldsymbol{v} \sim \mathcal{N}_c\left(\boldsymbol{0},\, \frac{E_1\,\sigma^2}{\eta_1^2} \cdot \boldsymbol{I}_2\right). \tag{61}$$

The corresponding bit estimates are given by

$$\begin{bmatrix} \hat{b}_{1,1} \\ \hat{b}_{2,1} \end{bmatrix} = \text{sign}\left(\Re\left\{\begin{bmatrix} d_{1,1} \\ d_{2,1} \end{bmatrix}\right\}\right). \tag{62}$$

The bit error probability is then given by

$$\begin{aligned}
P_1^{\mathrm{D}}(e) &= P(\Re\{d_{1,1}\} < 0 \,|\, b_{1,1} = +1) \\
&= P\left[E_1 + \mathcal{N}\left(0,\, \frac{E_1 \sigma^2}{2\eta_1^2}\right) < 0\right] \\
&= Q\left(\frac{\sqrt{2E_1}}{\sigma} \cdot \eta_1\right).
\end{aligned} \tag{63}$$

2) Linear Space–Time Multiuser Detector: We denote

$$\tilde{\boldsymbol{r}} \triangleq \begin{bmatrix} \boldsymbol{r}_1^{(1)} \\ \left(\boldsymbol{r}_2^{(1)}\right)^* \\ \boldsymbol{r}_1^{(2)} \\ \left(\boldsymbol{r}_2^{(2)}\right)^* \end{bmatrix}, \qquad \tilde{\boldsymbol{n}} \triangleq \begin{bmatrix} \boldsymbol{n}_1^{(1)} \\ \left(\boldsymbol{n}_2^{(1)}\right)^* \\ \boldsymbol{n}_1^{(2)} \\ \left(\boldsymbol{n}_2^{(2)}\right)^* \end{bmatrix}$$

$$\boldsymbol{h}_k \triangleq \begin{bmatrix} h_k^{(1,1)} \\ \left(h_k^{(2,1)}\right)^* \\ h_k^{(1,2)} \\ \left(h_k^{(2,2)}\right)^* \end{bmatrix}, \qquad \overline{\boldsymbol{h}}_k \triangleq \begin{bmatrix} h_k^{(2,1)} \\ \left(-h_k^{(1,1)}\right)^* \\ h_k^{(2,2)} \\ \left(-h_k^{(1,2)}\right)^* \end{bmatrix}.$$

Then, (47)–(50) may be written as

$$\tilde{\boldsymbol{r}} = \sum_{k=1}^{K} \left(b_{1,k} \boldsymbol{h}_k \otimes \boldsymbol{s}_k + b_{2,k} \overline{\boldsymbol{h}}_k \otimes \boldsymbol{s}_k\right) + \tilde{\boldsymbol{n}} = \tilde{\boldsymbol{S}} \boldsymbol{b} + \tilde{\boldsymbol{n}} \tag{64}$$

where

$$\tilde{\boldsymbol{S}} \triangleq \left[\boldsymbol{h}_1 \otimes \boldsymbol{s}_1,\ \overline{\boldsymbol{h}}_1 \otimes \boldsymbol{s}_1,\ \ldots,\ \boldsymbol{h}_K \otimes \boldsymbol{s}_K,\ \overline{\boldsymbol{h}}_K \otimes \boldsymbol{s}_K\right]_{4N \times 2K} \tag{65}$$

$$\boldsymbol{b} \triangleq [b_{1,1}\ b_{2,1}\ b_{1,2}\ b_{2,2} \cdots b_{1,K}\ b_{2,K}]^T. \tag{66}$$

Since $\boldsymbol{h}_k^H \overline{\boldsymbol{h}}_k = 0$ and (64) has the same form as (33), it is easy to show that the decorrelating detector for detecting the bit $b_{1,1}$ based on $\tilde{\boldsymbol{r}}$ is given by

$$\tilde{\boldsymbol{w}}_{1,1} = \frac{\boldsymbol{h}_1 \otimes \boldsymbol{w}_1}{\|\boldsymbol{h}_1\|^2}. \tag{67}$$

Hence, the output of the linear space–time detector in this case is given by

$$\tilde{z}_1 = \tilde{\boldsymbol{w}}_{1,1}^H \tilde{\boldsymbol{r}} = b_{1,1} + u_1 \tag{68}$$

with

$$u_1 \triangleq \tilde{\boldsymbol{w}}_{1,1}^H \tilde{\boldsymbol{n}} \sim \mathcal{N}_c(0,\, \sigma^2 \|\tilde{\boldsymbol{w}}_{1,1}\|^2) \tag{69}$$

where

$$\|\tilde{\boldsymbol{w}}_{1,1}\|^2 = \frac{\|\boldsymbol{w}_1\|^2}{\|\boldsymbol{h}_1\|^2} = \frac{1}{E_1 \eta_1^2}. \tag{70}$$

Therefore, the probability of detector error is given by

$$\begin{aligned}
P_1^{\mathrm{ST}}(e) &= P(\Re\{\tilde{z}_1\} < 0 \,|\, b_{1,1} = +1) \\
&= P\left[1 + \mathcal{N}\left(0,\, \frac{1}{2E_1 \eta_1^2}\right) < 0\right] \\
&= Q\left(\frac{\sqrt{2E_1}}{\sigma} \cdot \eta_1\right).
\end{aligned} \tag{71}$$

Comparing (71) with (63), it is seen that when two transmitter antennas and two receiver antennas are employed and the signals are transmitted in the form of space–time block code, then the linear diversity receiver and the linear space–time receiver have identical performance.

D. Remarks

We have seen that the performance of space–time multiuser detection (STMUD) and linear diversity multiuser detection (LDMUD) are similar for two transmit/one receive and two transmit/two receive antenna configurations. What, then, are the benefits of the space–time detection technique? They are as follows.

1) Although LDMUD and STMUD perform similarly for the 2–1 and 2–2 cases, the performance of STMUD is superior for configurations with one transmit antenna and $P \geq 2$ receive antennas.
2) User capacity for CDMA systems is limited by correlations among composite signature waveforms. This multiple-access interference will tend to decrease as the dimension of the vector space in which the signature waveforms reside increases. The signature waveforms for linear diversity detection are of length N, i.e., they reside in $\mathbb{C}^N$. Since the received signals are stacked for space–time detection, these signature waveforms reside in $\mathbb{C}^{2N}$ for two transmit and one receive antenna or $\mathbb{C}^{4N}$ for two transmit and two receive antennas. As a result, the space–time structure can support more users than linear diversity detection for a given performance threshold.
3) For adaptive configurations (Section III-1 and Section IV-D), LDMUD requires four independent subspace trackers operating simultaneously since the receiver performs detection on each of the four received signals, and each has a different signal subspace. The space–time structure requires only one subspace tracker.

III. Blind Adaptive Implementations of Space–Time Multiuser Detection for Synchronous CDMA

We next develop both batch and sequential *blind adaptive* implementations of the linear space–time receiver. These implementations are blind in the sense that they require only knowledge of the signature waveform of the user of interest. Instead of the decorrelating detector used for analysis in the previous section, we will use a linear MMSE detector for the adaptive implementations because the MMSE detector is more suitable for adaptation, and its performance is comparable with that of the decorrelating detector. This is reasonable since the detectors are asymptotically identical as the AWGN power tends to zero, and they share the same near–far resistance. We consider only the environment in which we have two transmitter antennas and two receiver antennas. The other cases can be derived in a similar manner. Note that inherent to any *blind* receiver in multiple transmitter antenna systems is an ambiguity issue. That is, if the same spreading waveform is used for a user at both transmitter antennas, the blind receiver cannot distinguish which bit is from which antenna. To resolve such an ambiguity, here, we use two different spreading waveforms for each user, i.e., $\boldsymbol{s}_{j,k}$, $j \in \{1, 2\}$ is the spreading code for user k for the transmission of bit $b_{j,k}$.

There are two bits $b_{1,k}[i]$ and $b_{2,k}[i]$ associated with each user at each time slot i, and the difference in time between slots is $2T_s$, where T_s is the symbol period. The received signal at antenna 1 during the two symbol periods for time slot i is

$$\boldsymbol{r}_1^{(1)}[i] = \sum_{k=1}^{K}\left(h_k^{(1,1)} b_{1,k}[i]\boldsymbol{s}_{1,k} + h_k^{(2,1)} b_{2,k}[i]\boldsymbol{s}_{2,k}\right) + \boldsymbol{n}_1^{(1)}[i] \tag{72}$$

$$\boldsymbol{r}_2^{(1)}[i] = \sum_{k=1}^{K}\left(-h_k^{(1,1)} b_{2,k}[i]\boldsymbol{s}_{2,k} + h_k^{(2,1)} b_{1,k}[i]\boldsymbol{s}_{1,k}\right) + \boldsymbol{n}_2^{(1)}[i] \tag{73}$$

and the corresponding signals received at antenna 2 are

$$\boldsymbol{r}_1^{(2)}[i] = \sum_{k=1}^{K}\left(h_k^{(1,2)} b_{1,k}[i]\boldsymbol{s}_{1,k} + h_k^{(2,2)} b_{2,k}[i]\boldsymbol{s}_{2,k}\right) + \boldsymbol{n}_1^{(2)}[i] \tag{74}$$

$$\boldsymbol{r}_2^{(2)}[i] = \sum_{k=1}^{K}\left(-h_k^{(1,2)} b_{2,k}[i]\boldsymbol{s}_{2,k} + h_k^{(2,2)} b_{1,k}[i]\boldsymbol{s}_{1,k}\right) + \boldsymbol{n}_2^{(2)}[i]. \tag{75}$$

We stack these received signal vectors and denote

$$\tilde{\boldsymbol{r}}[i] \triangleq \begin{bmatrix} \boldsymbol{r}_1^{(1)}[i] \\ \left(\boldsymbol{r}_2^{(1)}[i]\right)^* \\ \boldsymbol{r}_1^{(2)}[i] \\ \left(\boldsymbol{r}_2^{(2)}[i]\right)^* \end{bmatrix}, \qquad \tilde{\boldsymbol{n}}[i] \triangleq \begin{bmatrix} \boldsymbol{n}_1^{(1)}[i] \\ \left(\boldsymbol{n}_2^{(1)}[i]\right)^* \\ \boldsymbol{n}_1^{(2)}[i] \\ \left(\boldsymbol{n}_2^{(2)}[i]\right)^* \end{bmatrix}$$

$$\boldsymbol{h}_k \triangleq \begin{bmatrix} h_k^{(1,1)} \\ \left(h_k^{(2,1)}\right)^* \\ h_k^{(1,2)} \\ \left(h_k^{(2,2)}\right)^* \end{bmatrix}, \qquad \overline{\boldsymbol{h}}_k \triangleq \begin{bmatrix} h_k^{(2,1)} \\ \left(-h_k^{(1,1)}\right)^* \\ h_k^{(2,2)} \\ \left(-h_k^{(1,2)}\right)^* \end{bmatrix}.$$

Then, we may write

$$\begin{aligned}\tilde{\boldsymbol{r}}[i] &= \sum_{k=1}^{K}\left(b_{1,k}[i]\boldsymbol{h}_k \otimes \boldsymbol{s}_{1,k} + b_{2,k}[i]\overline{\boldsymbol{h}}_k \otimes \boldsymbol{s}_{2,k}\right) + \tilde{\boldsymbol{n}}[i] \\ &= \tilde{\boldsymbol{S}}\boldsymbol{b}[i] + \tilde{\boldsymbol{n}}[i]\end{aligned} \tag{76}$$

where

$$\begin{aligned}\tilde{\boldsymbol{S}} &\triangleq \big[\boldsymbol{h}_1 \otimes \boldsymbol{s}_{1,1},\, \overline{\boldsymbol{h}}_1 \otimes \boldsymbol{s}_{2,1} \\ &\qquad \ldots \boldsymbol{h}_K \otimes \boldsymbol{s}_{1,K},\, \overline{\boldsymbol{h}}_K \otimes \boldsymbol{s}_{2,K}\big]_{4N\times 2K} \\ \boldsymbol{b}[i] &\triangleq [b_{1,1}[i]\; b_{2,1}[i]\; b_{1,2}[i]\; b_{2,2}[i] \cdots b_{1,K}[i]\; b_{2,K}[i]]^T_{2K\times 1}.\end{aligned}$$

The autocorrelation matrix $\boldsymbol{C}$ of the stacked signal $\tilde{\boldsymbol{r}}[i]$ and its eigendecomposition are given by

$$\boldsymbol{C} = E\{\tilde{\boldsymbol{r}}[i]\tilde{\boldsymbol{r}}[i]^H\} = \tilde{\boldsymbol{S}}\tilde{\boldsymbol{S}}^H + \sigma^2\boldsymbol{I}_{4N} \tag{77}$$

$$= \boldsymbol{U}_s\boldsymbol{\Lambda}_s\boldsymbol{U}_s^H + \sigma^2\boldsymbol{U}_n\boldsymbol{U}_n^H \tag{78}$$

where $\boldsymbol{\Lambda}_s = \mathrm{diag}\{\lambda_1, \lambda_2, \ldots, \lambda_{2K}\}$ contains the largest $(2K)$ eigenvalues of $\boldsymbol{C}$, the columns of $\boldsymbol{U}_s$ are the corresponding eigenvectors; and the columns of $\boldsymbol{U}_n$ are the $(4N-2K)$ eigenvectors corresponding to the smallest eigenvalue σ^2.

The blind linear MMSE detector for detecting $[\boldsymbol{b}[i]]_1 = b_{1,1}[i]$ is given by the solution to the optimization problem

$$\boldsymbol{w}_{1,1} \triangleq \arg \min_{\boldsymbol{w}\in\mathcal{C}^{4N}} \mathrm{E}\{|b_{1,1}[i] - \boldsymbol{w}^H\tilde{\boldsymbol{r}}[i]|^2\}. \tag{79}$$

It has been shown in [23] that a scaled version of the solution can be written in terms of the signal subspace components as

$$\boldsymbol{w}_{1,1} = \boldsymbol{U}_s\boldsymbol{\Lambda}_s^{-1}\boldsymbol{U}_s^H(\boldsymbol{h}_1 \otimes \boldsymbol{s}_{1,1}) \tag{80}$$

and the decision is made according to

$$z_{1,1}[i] = \boldsymbol{w}_{1,1}^H\tilde{\boldsymbol{r}}[i] \tag{81}$$
$$\hat{b}_{1,1}[i] = \mathrm{sign}[\Re(z_{1,1}[i])] \quad \text{(coherent detection)} \tag{82}$$
$$\hat{\beta}_{1,1}[i] = \mathrm{sign}[\Re(z_{1,1}[i-1]^* z_{1,1}[i])] \quad \text{(differential detection).} \tag{83}$$

Before we address specific batch and sequential adaptive algorithms, we note that these algorithms can be also be implemented using linear *group-blind* multiuser detectors instead of blind MMSE detectors. This would be appropriate, for example, in uplink environments in which the base station has knowledge of the signature waveforms of all of the users in the cell but not those of users outside the cell. Specifically, we may rewrite (76) as

$$\tilde{\boldsymbol{r}}[i] = \breve{\boldsymbol{S}}\breve{\boldsymbol{b}}[i] + \overline{\boldsymbol{S}}\overline{\boldsymbol{b}}[i] + \tilde{\boldsymbol{n}}[i] \tag{84}$$

where we have separated the users into two groups. The composite signature sequences of the known users are the columns of $\breve{\boldsymbol{S}}$. The unknown users' composite sequences are the columns of $\overline{\boldsymbol{S}}$. Then, the group-blind linear hybrid detector for bit $b_{1,1}[i]$ is given by [24]

$$\boldsymbol{w}_{1,1}^{\mathrm{GB}} = \boldsymbol{U}_s\boldsymbol{\Lambda}_s^{-1}\boldsymbol{U}_s^H\breve{\boldsymbol{S}}\left[\breve{\boldsymbol{S}}^H\boldsymbol{U}_s\boldsymbol{\Lambda}_s^{-1}\boldsymbol{U}_s^H\breve{\boldsymbol{S}}\right]^{-1}(\boldsymbol{h}_1\otimes\boldsymbol{s}_{1,1}). \tag{85}$$

This detector offers a significant performance improvement over blind implementations of (80) for environments in which the signature sequences of some of the interfering users are known.

1) Batch Blind Linear Space–Time Multiuser Detection: In order to obtain an estimate of $\boldsymbol{h}_1$, we make use of the orthogonality between the signal and noise subspaces, i.e., the fact that $\boldsymbol{U}_n^H(\boldsymbol{h}_1 \otimes \boldsymbol{s}_{1,1}) = \boldsymbol{0}$. In particular, we have

$$\begin{aligned}\hat{\boldsymbol{h}}_1 &= \arg\min_{\boldsymbol{h}\in\mathcal{C}^4} ||\boldsymbol{U}_n^H(\boldsymbol{h}\otimes\boldsymbol{s}_{1,1})||^2\\ &= \arg\max_{\boldsymbol{h}\in\mathcal{C}^4} ||\boldsymbol{U}_s^H(\boldsymbol{h}\otimes\boldsymbol{s}_{1,1})||^2\\ &= \arg\max_{\boldsymbol{h}\in\mathcal{C}^4} (\boldsymbol{h}^H\otimes\boldsymbol{s}_{1,1}^T)\boldsymbol{U}_s\boldsymbol{U}_s^H(\boldsymbol{h}\otimes\boldsymbol{s}_{11})\\ &= \arg\max_{\boldsymbol{h}\in\mathcal{C}^4} \boldsymbol{h}^H\underbrace{[(\boldsymbol{I}_4\otimes\boldsymbol{s}_{1,1}^T)\boldsymbol{U}_s\boldsymbol{U}_s^H(\boldsymbol{I}_4\otimes\boldsymbol{s}_{1,1})]}_{\boldsymbol{Q}}\boldsymbol{h} \qquad (86)\\ &= \text{principle eigenvector of } \boldsymbol{Q}. \qquad (87)\end{aligned}$$

In (87), $\hat{\boldsymbol{h}}_1$ specifies $\boldsymbol{h}_1$ up to an arbitrary complex scale factor α, i.e., $\hat{\boldsymbol{h}}_1 = \alpha\boldsymbol{h}_1$. The following is the summary of a batch blind space–time multiuser detection algorithm for the two transmitter antenna/two receiver antenna configuration. The block length is M.

Algorithm 1 [Batch Blind Linear Space–Time Multiuser Detector—Synchronous CDMA, Two Transmitter Antennas and Two Receiver Antennas]:

- Estimate the signal subspace

$$\begin{aligned}\hat{\boldsymbol{C}} &= \frac{1}{M}\sum_{i=0}^{M-1}\tilde{\boldsymbol{r}}[i]\tilde{\boldsymbol{r}}[i]^H \qquad (88)\\ &= \hat{\boldsymbol{U}}_s\hat{\boldsymbol{\Lambda}}_s\hat{\boldsymbol{U}}_s^H + \hat{\boldsymbol{U}}_n\hat{\boldsymbol{\Lambda}}_n\hat{\boldsymbol{U}}_n^H. \qquad (89)\end{aligned}$$

- Estimate the channels

$$\hat{\boldsymbol{Q}}_1 = (\boldsymbol{I}_4\otimes\boldsymbol{s}_{1,1}^T)\hat{\boldsymbol{U}}_s\hat{\boldsymbol{U}}_s^H(\boldsymbol{I}_4\otimes\boldsymbol{s}_{1,1}) \tag{90}$$
$$\hat{\boldsymbol{Q}}_2 = (\boldsymbol{I}_4\otimes\boldsymbol{s}_{2,1}^T)\hat{\boldsymbol{U}}_s\hat{\boldsymbol{U}}_s^H(\boldsymbol{I}_4\otimes\boldsymbol{s}_{2,1}) \tag{91}$$
$$\hat{\boldsymbol{h}}_1 = \text{principal eigenvector of } \hat{\boldsymbol{Q}}_1 \tag{92}$$
$$\hat{\overline{\boldsymbol{h}}}_1 = \text{principal eigenvector of } \hat{\boldsymbol{Q}}_2. \tag{93}$$

- Form the detectors

$$\hat{\boldsymbol{w}}_{1,1} = \hat{\boldsymbol{U}}_s\hat{\boldsymbol{\Lambda}}_s^{-1}\hat{\boldsymbol{U}}_s^H\left(\hat{\boldsymbol{h}}_1\otimes\boldsymbol{s}_{1,1}\right) \tag{94}$$
$$\hat{\boldsymbol{w}}_{2,1} = \hat{\boldsymbol{U}}_s\hat{\boldsymbol{\Lambda}}_s^{-1}\hat{\boldsymbol{U}}_s^H\left(\hat{\overline{\boldsymbol{h}}}_1\otimes\boldsymbol{s}_{2,1}\right). \tag{95}$$

- Perform differential detection

$$z_{1,1}[i] = \hat{\boldsymbol{w}}_{1,1}^H\tilde{\boldsymbol{r}}[i] \tag{96}$$
$$z_{2,1}[i] = \hat{\boldsymbol{w}}_{2,1}^H\tilde{\boldsymbol{r}}[i], \tag{97}$$
$$\hat{\beta}_{1,1}[i] = \mathrm{sign}(\Re\{z_{1,1}[i]z_{1,1}[i-1]^*\}) \tag{98}$$
$$\hat{\beta}_{2,1}[i] = \mathrm{sign}(\Re\{z_{2,1}[i]z_{2,1}[i-1]^*\}) \quad i = 0, \ldots, M-1. \tag{99}$$

A batch group-blind space–time multiuser detector algorithm can be implemented with simple modifications to (94) and (95).

2) Adaptive Blind Linear Space–Time Multiuser Detection: To form a sequential blind adaptive receiver, we need adaptive algorithms for sequentially estimating the channel and the signal subspace components $\boldsymbol{U}_s$ and $\boldsymbol{\Lambda}_s$. First, we address sequential adaptive channel estimation. Denote by $\boldsymbol{z}[i]$ the projection of the stacked signal $\tilde{\boldsymbol{r}}[i]$ onto the noise subspace, i.e.,

$$\begin{aligned}\boldsymbol{z}[i] &= \tilde{\boldsymbol{r}}[i] - \boldsymbol{U}_s\boldsymbol{U}_s^H\tilde{\boldsymbol{r}}[i] \qquad (100)\\ &= \boldsymbol{U}_n\boldsymbol{U}_n^H\tilde{\boldsymbol{r}}[i]. \qquad (101)\end{aligned}$$

Since $\boldsymbol{z}[i]$ lies in the noise subspace, it is orthogonal to any signal in the signal subspace, and, in particular, it is orthogonal to $(\boldsymbol{h}_1\otimes\boldsymbol{s}_{1,1})$. Hence, $\boldsymbol{h}_1$ is the solution to the following constrained optimization problem:

$$\begin{aligned}&\min_{\boldsymbol{h}_1\in\mathcal{C}^4} E\{||\boldsymbol{z}[i]^H(\boldsymbol{h}_1\otimes\boldsymbol{s}_{1,1})||^2\}\\ &= \min_{\boldsymbol{h}_1\in\mathcal{C}^4} E\{||\boldsymbol{z}[i]^H(\boldsymbol{I}_4\otimes\boldsymbol{s}_{1,1})\boldsymbol{h}_1||^2\}\\ &= \min_{\boldsymbol{h}_1\in\mathcal{C}^4} E\{||[(\boldsymbol{I}_4\otimes\boldsymbol{s}_{1,1}^T)\boldsymbol{z}[i]]^H\boldsymbol{h}_1||^2\}\\ &\quad \text{s.t. } ||\boldsymbol{h}_1|| = 1. \qquad (102)\end{aligned}$$

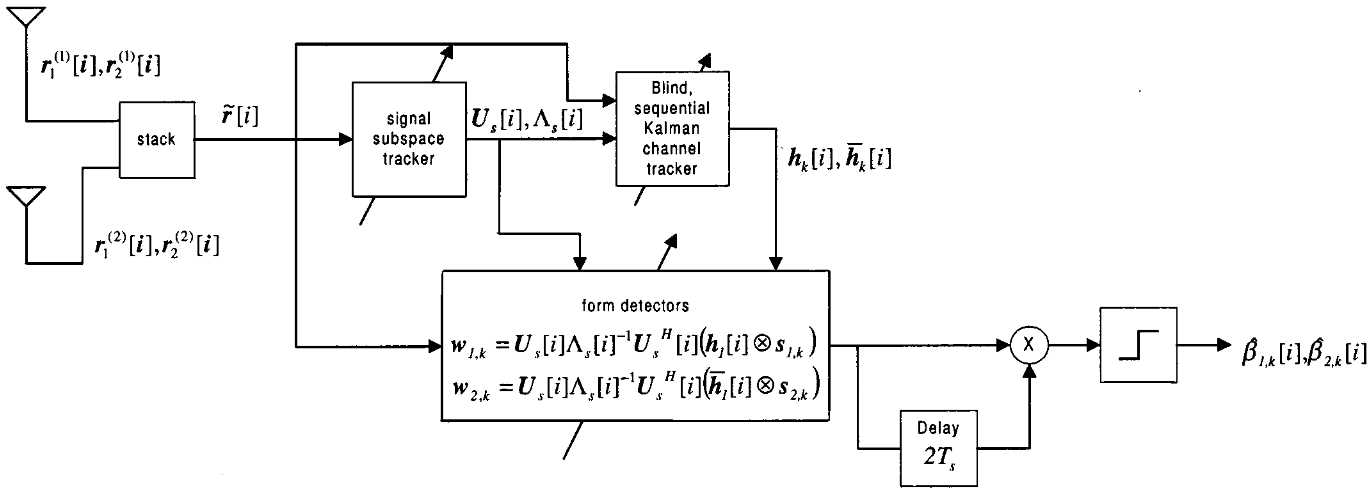

Fig. 1. Adaptive receiver structure for linear space–time multiuser detectors.

In order to obtain a sequential algorithm to solve the above optimization problem, we write it in the following (trivial) state-space form:

$$\boldsymbol{h}_1[i+1] = \boldsymbol{h}_1[i], \quad \text{state equation}$$
$$0 = [(\boldsymbol{I}_4 \otimes \boldsymbol{s}_{1,1}^T)\boldsymbol{z}[i]]^H \boldsymbol{h}_1[i], \quad \text{observation equation.}$$

The standard Kalman filter can then be applied to the above system as follows. Denote $\boldsymbol{x}[i] \triangleq (\boldsymbol{I}_4 \otimes \boldsymbol{s}_{1,1}^T)\boldsymbol{z}[i]$.

$$\boldsymbol{k}[i] = \boldsymbol{\Sigma}[i-1]\boldsymbol{x}[i](\boldsymbol{x}[i]^H\boldsymbol{\Sigma}[i-1]\boldsymbol{x}[i])^{-1} \tag{103}$$
$$\boldsymbol{h}_1[i] = \boldsymbol{h}_1[i-1] - \boldsymbol{k}[i](\boldsymbol{x}[i]^H\boldsymbol{h}_1[i-1]) \\ /||\boldsymbol{h}_1[i-1] - \boldsymbol{k}[i](\boldsymbol{x}[i]^H\boldsymbol{h}_1[i-1])|| \tag{104}$$
$$\boldsymbol{\Sigma}[i] = \boldsymbol{\Sigma}[i-1] - \boldsymbol{k}[i]\boldsymbol{x}[i]^H\boldsymbol{\Sigma}[i-1]. \tag{105}$$

Once we have obtained channel estimates at time slot i, we can combine them with estimates of the signal subspace components to form the detector in (80). Subspace tracking algorithms of various complexities exist in the literature. Since we are stacking received signal vectors and subspace tracking complexity increases at least linearly with signal subspace dimension, it is imperative that we choose an algorithm with minimal complexity. The best existing low-complexity algorithm for this purpose appears to be NAHJ-FST. This algorithm has the lowest complexity of any algorithm used for similar purposes and has performed well when used for signal subspace tracking in multipath fading environments. Since the size of $\boldsymbol{U}_s$ is $4N \times 2K$, the complexity is $40 \cdot 4N \cdot 2K + 3 \cdot 4N + 7.5(2K)^2 + 7 \cdot 2K$ floating operations per iteration. The algorithm and a multiuser detection application are presented in [25]. The application to the current tracking problem is straightforward and will not be discussed in detail.

Algorithm 2 [Blind Adaptive Linear Space–Time Multiuser Detector—Synchronous CDMA, Two Transmitter Antennas and Two Receiver Antennas]:

- Using a suitable signal subspace tracking algorithm, e.g., NAHJ-FST, update the signal subspace components $\boldsymbol{U}_s[i]$ and $\boldsymbol{\Lambda}_s[i]$ at each time slot i
- Track the channel $\boldsymbol{h}_1[i]$ and $\overline{\boldsymbol{h}}_1[i]$ according to the following:

$$\boldsymbol{z}[i] = \tilde{\boldsymbol{r}}[i] - \boldsymbol{U}_s[i]\boldsymbol{U}_s[i]^H\tilde{\boldsymbol{r}}[i] \tag{106}$$
$$\boldsymbol{x}[i] = (\boldsymbol{I}_4 \otimes \boldsymbol{s}_{1,1}^T)\boldsymbol{z}[i] \tag{107}$$
$$\overline{\boldsymbol{x}}[i] = (\boldsymbol{I}_4 \otimes \boldsymbol{s}_{2,1}^T)\boldsymbol{z}[i] \tag{108}$$
$$\boldsymbol{k}[i] = \boldsymbol{\Sigma}[i-1]\boldsymbol{x}[i](\boldsymbol{x}[i]^H\boldsymbol{\Sigma}[i-1]\boldsymbol{x}[i])^{-1} \tag{109}$$
$$\overline{\boldsymbol{k}}[i] = \overline{\boldsymbol{\Sigma}}[i-1]\overline{\boldsymbol{x}}[i]\left(\overline{\boldsymbol{x}}[i]^H\overline{\boldsymbol{\Sigma}}[i-1]\overline{\boldsymbol{x}}[i]\right)^{-1} \tag{110}$$
$$\boldsymbol{h}_1[i] = \boldsymbol{h}_1[i-1] - \boldsymbol{k}[i](\boldsymbol{x}[i]^H\boldsymbol{h}_1[i-1]) \\ /||\boldsymbol{h}_1[i-1] - \boldsymbol{k}[i](\boldsymbol{x}[i]^H\boldsymbol{h}_1[i-1])|| \tag{111}$$
$$\overline{\boldsymbol{h}}_1[i] = \overline{\boldsymbol{h}}_1[i-1] - \overline{\boldsymbol{k}}[i](\overline{\boldsymbol{x}}[i]^H\overline{\boldsymbol{h}}_1[i-1]) \\ /\left\|\overline{\boldsymbol{h}}_1[i-1] - \overline{\boldsymbol{k}}[i]\left(\overline{\boldsymbol{x}}[i]^H\overline{\boldsymbol{h}}_1[i-1]\right)\right\| \tag{112}$$
$$\boldsymbol{\Sigma}[i] = \boldsymbol{\Sigma}[i-1] - \boldsymbol{k}[i]\boldsymbol{x}[i]^H\boldsymbol{\Sigma}[i-1] \tag{113}$$
$$\overline{\boldsymbol{\Sigma}}[i] = \overline{\boldsymbol{\Sigma}}[i-1] - \overline{\boldsymbol{k}}[i]\overline{\boldsymbol{x}}[i]^H\overline{\boldsymbol{\Sigma}}[i-1]. \tag{114}$$

- Form the detectors

$$\hat{\boldsymbol{w}}_{1,1}[i] = \boldsymbol{U}_s[i]\boldsymbol{\Lambda}_s^{-1}[i]\boldsymbol{U}_s[i]^H(\boldsymbol{h}_1[i] \otimes \boldsymbol{s}_{1,1}) \tag{115}$$
$$\hat{\boldsymbol{w}}_{2,1}[i] = \boldsymbol{U}_s[i]\boldsymbol{\Lambda}_s^{-1}[i]\boldsymbol{U}_s[i]^H\left(\overline{\boldsymbol{h}}_1[i] \otimes \boldsymbol{s}_{2,1}\right). \tag{116}$$

- Perform differential detection

$$z_{1,1}[i] = \hat{\boldsymbol{w}}_{1,1}[i]^H\tilde{\boldsymbol{r}}[i] \tag{117}$$
$$z_{2,1}[i] = \hat{\boldsymbol{w}}_{2,1}[i]^H\tilde{\boldsymbol{r}}[i] \tag{118}$$
$$\hat{\beta}_{1,1}[i] = \text{sign}(\Re\{z_{1,1}[i]z_{1,1}[i-1]^*\}) \tag{119}$$
$$\hat{\beta}_{2,1}[i] = \text{sign}(\Re\{z_{2,1}[i]z_{2,1}[i-1]^*\}). \tag{120}$$

A group-blind sequential adaptive space–time multiuser detector can be implemented similarly. The adaptive receiver structure is illustrated in Fig. 1.

IV. Blind Adaptive Space–Time Multiuser Detection for Asynchronous CDMA in Fading Multipath Channels

A. Signal Model

In this section, we develop adaptive space–time multiuser detectors for asynchronous CDMA systems with two transmitter and two receiver antennas. The continuous-time signal transmitted from antennas 1 and 2 due to the kth user for time interval $i \in \{0, 1, \ldots\}$ is given by

$$x_k^{(1)}(t) = \sum_{i=0}^{M-1} [b_{1,k}[i]s_{1,k}(t-2iT_s) - b_{2,k}[i]s_{2,k}(t-(2i+1)T_s)] \quad (121)$$

$$x_k^{(2)}(t) = \sum_{i=0}^{M-1} [b_{2,k}[i]s_{2,k}(t-2iT_s) + b_{1,k}[i]s_{1,k}(t-(2i+1)T_s)] \quad (122)$$

where

M length of the data frame;
T_s information symbol interval;
$\{b_k[i]\}_i$ symbol stream of user k.

Although this is an asynchronous system, we have, for notational simplicity, suppressed the delay associated with each users' signal and incorporated it into the path delays in (124). We assume that for each k, the symbol stream $\{b_k[i]\}_i$ is a collection of independent random variables that take on values of $+1$ and -1 with equal probability. Furthermore, we assume that the symbol streams of different users are independent. For the direct-sequence spread-spectrum (DS-SS) format, the user signaling waveforms have the form

$$s_{q,k}(t) = \sum_{j=0}^{N-1} c_{q,k}[j]\psi(t-jT_c), \qquad 0 \le t \le T \quad (123)$$

where

N processing gain;
$\{c_{q,k}[j]\}_i,\ q \in \{1, 2\}$ signature sequence of ± 1s assigned to the kth user for bit $b_{q,k}[i]$;
$\psi(t)$ normalized chip waveform of duration $T_c = T_s/N$.

The kth user's signals $x_k^{(1)}(t)$ and $x_k^{(2)}(t)$ propagate from transmitter antenna a to receiver antenna b through a multipath fading channel whose impulse response is given by

$$g_k^{(a,b)}(t) = \sum_{l=1}^{L} \alpha_{kl}^{(a,b)} \delta\left(t - \tau_{kl}^{(a,b)}\right) \quad (124)$$

where $\alpha_{kl}^{(a,b)}$ is the complex path gain from antenna a to antenna b associated with the lth path for the kth user, and $\tau_{kl}^{(a,b)}$, $\tau_{k1}^{(a,b)} < \tau_{k2}^{(a,b)} < \cdots < \tau_{kL}^{(a,b)}$ is the sum of the corresponding path delay and the initial transmission delay of user k. It is assumed that the channel is slowly varying so that the path gains and delays remain constant over the duration of one signal frame (MT_s).

The received signal component due to the transmission of $x_k^{(1)}(t)$ and $x_k^{(2)}(t)$ through the channel at receiver antennas 1 and 2 is given by

$$y_k^{(1)}(t) = x_k^{(1)}(t) \star g_k^{(1,1)}(t) + x_k^{(2)}(t) \star g_k^{(2,1)}(t) \quad (125)$$

$$y_k^{(2)}(t) = x_k^{(1)}(t) \star g_k^{(1,2)}(t) + x_k^{(2)}(t) \star g_k^{(2,2)}(t). \quad (126)$$

Substituting (121), (122), and (124) into (125) and (126), we have for receiver antenna $b \in \{1, 2\}$

$$\begin{aligned} y_k^{(b)}(t) = &\sum_{i=0}^{M-1} \Big[b_{1,k}[i]s_{1,k}(t-2iT_s) \star g_k^{(1,b)}(t) \\ &- b_{2,k}[i]s_{2,k}(t-(2i+1)T_s) \star g_k^{(1,b)}(t)\Big] \\ &+ \sum_{i=0}^{M-1} \Big[b_{2,k}[i]s_{2,k}(t-2iT_s) \star g_k^{(2,b)}(t) \\ &+ b_{1,k}[i]s_{1,k}(t-(2i+1)T_s) \star g_k^{(2,b)}(t)\Big]. \end{aligned} \quad (127)$$

For $a, b, q \in \{1, 2\}$, we define

$$\begin{aligned} h_{q,k}^{(a,b)}(t) &\triangleq s_{q,k}(t) \star g_k^{(a,b)}(t) \\ &= \sum_{j=0}^{N-1} c_{q,k}[j] \underbrace{\left[\sum_{l=1}^{L} \alpha_{kl}^{(a,b)} \psi\left(t - jT_c - \tau_{kl}^{(a,b)}\right)\right]}_{\overline{g}_k^{(a,b)}(t-jT_c)}. \end{aligned} \quad (128)$$

In (128), $\overline{g}_k^{(a,b)}(t)$ is the composite channel response for the channel between transmitter antenna a and receiver antenna b, taking into account the effects of the chip pulse waveform and the multipath channel. Then, we have

$$\begin{aligned} y_k^{(b)}(t) = &\sum_{i=0}^{M-1} \Big[b_{1,k}[i]h_{1,k}^{(1,b)}(t-2iT_s) \\ &- b_{2,k}[i]h_{2,k}^{(1,b)}(t-(2i+1)T_s)\Big] \\ &+ \sum_{i=0}^{M-1} \Big[b_{2,k}[i]h_{2,k}^{(2,b)}(t-2iT_s) \\ &+ b_{1,k}[i]h_{1,k}^{(2,b)}(t-(2i+1)T_s)\Big]. \end{aligned} \quad (129)$$

The total received signal at receiver antenna $b \in \{1, 2\}$ is given by

$$r^{(b)}(t) = \sum_{k=1}^{K} y_k^{(b)}(t) + v^{(b)}(t). \quad (130)$$

At the receiver, the received signal is match filtered to the chip waveform and sampled at the chip rate, i.e., the sampling interval is T_c, N is the total number of samples per symbol interval, and $2N$ is the total number of samples per time slot. The nth matched filter output during the ith time slot is given by

$$\begin{aligned} r^{(b)}[i, n] &\triangleq \int_{2iT_s+nT_c}^{2iT_s+(n+1)T_c} r^{(b)}(t)\psi(t-2iT_s-nT_c)\,\mathrm{d}t \\ &= \sum_{k=1}^{K} \underbrace{\left\{\int_{2iT_s+nT_c}^{2iT_s+(n+1)T_c} \psi(t-2iT_s-nT_c)y_k^{(b)}(t)\,\mathrm{d}t\right\}}_{y_k^{(b)}[i,n]} \\ &\quad + \underbrace{\int_{2iT_s+nT_c}^{2iT_s+(n+1)T_c} v^{(b)}(t)\psi(t-2iT_s-nT_c)\,\mathrm{d}t}_{v^{(b)}[i,n]}. \end{aligned} \tag{131}$$

Denote the maximum delay (in symbol intervals) as

$$\iota_k^{(a,b)} \triangleq \left\lceil \frac{\tau_{kL}^{(a,b)} + T_c}{T_s} \right\rceil \quad \text{and} \quad \iota \triangleq \max_{k,a,b} \iota_k^{(a,b)}. \tag{132}$$

Substituting (129) into (131), we obtain

$$\begin{aligned} y_k^{(b)}[i, n] = \sum_{p=0}^{M-1} \Bigg\{ & b_{1,k}[p] \int_{2iT_s+nT_c}^{2iT_s+(n+1)T_c} h_{1,k}^{(1,b)}(t-2pT_s) \\ & \cdot \psi(t-2iT_s-nT_c)\,\mathrm{d}t \\ & - b_{2,k}[p] \int_{2iT_s+nT_c}^{2iT_s+(n+1)T_c} h_{2,k}^{(1,b)}(t-(2p+1)T_s) \\ & \cdot \psi(t-2iT_s-nT_c)\,\mathrm{d}t \\ & + b_{2,k}[p] \int_{2iT_s+nT_c}^{2iT_s+(n+1)T_c} h_{2,k}^{(2,b)}(t-2pT_s) \\ & \cdot \psi(t-2iT_s-nT_c)\,\mathrm{d}t \\ & + b_{1,k}[p] \int_{2iT_s+nT_c}^{2iT_s+(n+1)T_c} h_{1,k}^{(2,b)}(t-(2p-1)T_s) \\ & \cdot \psi(t-2iT_s-nT_c)\,\mathrm{d}t \Bigg\}. \end{aligned} \tag{133}$$

Further substitution of (128) into (133) is as in (134), shown at the bottom of the next page. We may write $y_k^{(b)}[i, n]$ more compactly as

$$\begin{aligned} y_k^{(b)}[i, n] &= \sum_{j=0}^{\lceil \iota/2 \rceil} \Big(h_{1,k}^{(1,b)}[j, n] b_{1,k}[i-j] - h_{2,k}^{(1,b)}[j, n] b_{2,k}[i-j] \\ &\qquad + h_{2,k}^{(2,b)}[j, n] b_{2,k}[i-j] + h_{1,k}^{(2,b)}[j, n] b_{1,k}[i-j] \Big) \\ &= \sum_{j=0}^{\lceil \iota/2 \rceil} b_{1,k}[i-j] g_{1,k}^{(b)}[j, n] + \sum_{j=0}^{\lceil \iota/2 \rceil} b_{2,k}[i-j] g_{2,k}^{(b)}[j, n] \end{aligned} \tag{135}$$

where

$$g_{1,k}^{(b)}[j, n] \triangleq h_{1,k}^{(1,b)}[j, n] + h_{1,k}^{(2,b)}[j, n] \tag{136}$$

$$g_{2,k}^{(b)}[j, n] \triangleq h_{2,k}^{(2,b)}[j, n] - h_{2,k}^{(1,b)}[j, n]. \tag{137}$$

For $j = 0, 1, \ldots, \lceil \iota/2 \rceil$, we have (138), shown at the bottom of the next page, and

$$\begin{aligned} \underline{r}^{(b)}[i] &\triangleq \begin{bmatrix} r^{(b)}[i, 0] \\ \vdots \\ r^{(b)}[i, 2N-1] \end{bmatrix}_{2N\times 1} \\ \underline{v}^{(b)}[i] &\triangleq \begin{bmatrix} v^{(b)}[i, 0] \\ \vdots \\ v^{(b)}[i, 2N-1] \end{bmatrix}_{2N\times 1} \\ \underline{b}[i] &\triangleq \begin{bmatrix} b_{1,1}[i] \\ \vdots \\ b_{1,K}[i] \\ b_{2,1}[i] \\ \vdots \\ b_{2,K}[i] \end{bmatrix}_{2K\times 1}. \end{aligned} \tag{139}$$

Then, we have

$$\underline{r}^{(b)}[i] = \underbrace{\sum_{j=0}^{\lceil \iota/2 \rceil} \underline{H}^{(b)}[j] \underline{b}[i-j]}_{\underline{H}^{(b)}[i] \star \underline{b}[i]} + \underline{v}^{(b)}[i]. \tag{140}$$

To exploit both time and spatial diversity, we stack the vectors received from both receive antennas

$$\underline{r}[i] \triangleq \begin{bmatrix} \underline{r}^{(1)}[i] \\ \underline{r}^{(2)}[i] \end{bmatrix}_{4N\times 1} \tag{141}$$

and observe that

$$\underline{r}[i] = \underline{H}[i] \star \underline{b}[i] + \underline{v}[i] \tag{142}$$

where

$$\underline{H}[j] \triangleq \begin{bmatrix} \underline{H}^{(1)}[j] \\ \underline{H}^{(2)}[j] \end{bmatrix}_{4N\times 2K}, \qquad j = 0, 1, \ldots, \lceil \iota/2 \rceil$$

and

$$\underline{v}[i] \triangleq \begin{bmatrix} \underline{v}^{(1)}[i] \\ \underline{v}^{(2)}[i] \end{bmatrix}_{4N\times 1}. \tag{143}$$

By stacking m successive received sample vectors, we create the following quantities:

$$\begin{aligned} \boldsymbol{r}[i] &\triangleq \begin{bmatrix} \underline{r}[i] \\ \vdots \\ \underline{r}[i+m-1] \end{bmatrix}_{4Nm\times 1} \\ \boldsymbol{v}[i] &\triangleq \begin{bmatrix} \underline{v}[i] \\ \vdots \\ \underline{v}[i+m-1] \end{bmatrix}_{4Nm\times 1} \\ \boldsymbol{b}[i] &\triangleq \begin{bmatrix} \underline{b}[i-\lceil \iota/2 \rceil] \\ \vdots \\ \underline{b}[i+m-1] \end{bmatrix}_{r\times 1} \end{aligned} \tag{144}$$

$$\boldsymbol{H} \triangleq \begin{bmatrix} \underline{H}[\lceil \iota/2 \rceil] & \cdots & \underline{H}[0] & \cdots & \mathbf{0} \\ \vdots & \ddots & \ddots & \ddots & \vdots \\ \mathbf{0} & \cdots & \underline{H}[\lceil \iota/2 \rceil] & \cdots & \underline{H}[0] \end{bmatrix}_{4Nm \times r} \tag{145}$$

where $r \triangleq 2K(m + \lceil \iota/2 \rceil)$. We can write (142) in matrix form as

$$\boldsymbol{r}[i] = \boldsymbol{H}\boldsymbol{b}[i] + \boldsymbol{v}[i]. \tag{146}$$

We will see in Section IV-C2 that the smoothing factor m is chosen such that

$$m \geq \left\lceil \frac{N(\iota+1) + K\lceil \iota/2 \rceil + 1}{2N - K} \right\rceil \tag{147}$$

for channel identifiability. Note that the columns of $\boldsymbol{H}$ (the composite signature vectors) contain information about both the timings and the complex path gains of the multipath channel of each user. Hence, an estimate of these waveforms eliminates the need for separate estimates of the timing information $\{\tau_{kl}^{(a,b)}\}_{l=1}^{L}$.

$$\begin{aligned} y_k^{(b)}[i, n] = \sum_{p=0}^{M-1} \Bigg\{ & b_{1,k}[p] \sum_{j=0}^{N-1} c_{1,k}[j] \sum_{l=1}^{L} \alpha_{kl}^{(1,b)} \int_{2iT_s+nT_c}^{2iT_s+(n+1)T_c} \psi(t - 2iT_s - nT_c)\psi\left(t - 2pT_s - jT_c - \tau_{kl}^{(1,b)}\right) \mathrm{d}t \\ & - b_{2,k}[p] \sum_{j=0}^{N-1} c_{2,k}[j] \sum_{l=1}^{L} \alpha_{kl}^{(1,b)} \int_{2iT_s+nT_c}^{2iT_s+(n+1)T_c} \psi(t - 2iT_s - nT_c)\psi\left(t - (2p+1)T_s - jT_c - \tau_{kl}^{(1,b)}\right) \mathrm{d}t \\ & + b_{2,k}[p] \sum_{j=0}^{N-1} c_{2,k}[j] \sum_{l=1}^{L} \alpha_{kl}^{(2,b)} \int_{2iT_s+nT_c}^{2iT_s+(n+1)T_c} \psi(t - 2iT_s - nT_c)\psi\left(t - 2pT_s - jT_c - \tau_{kl}^{(2,b)}\right) \mathrm{d}t \\ & + b_{1,k}[p] \sum_{j=0}^{N-1} c_{1,k}[j] \sum_{l=1}^{L} \alpha_{kl}^{(2,b)} \int_{2iT_s+nT_c}^{2iT_s+(n+1)T_c} \psi(t - 2iT_s - nT_c)\psi\left(t - (2p+1)T_s - jT_c - \tau_{kl}^{(2,b)}\right) \mathrm{d}t \Bigg\} \\ = \sum_{p=0}^{\lceil \iota/2 \rceil} \Bigg\{ & b_{1,k}[i-p] \underbrace{\sum_{j=0}^{N-1} c_{1,k}[j] \overbrace{\sum_{l=1}^{L} \alpha_{kl}^{(1,b)} \int_0^{T_c} \psi(t)\psi\left(t - jT_c - \tau_{kl}^{(1,b)} + 2pT_s + nT_c\right) \mathrm{d}t]}^{f_k^{(1,b)}[n+2pN-j]}}_{h_{1,k}^{(1,b)}[p,n]} \\ & - b_{2,k}[i-p] \underbrace{\sum_{j=0}^{N-1} c_{2,k}[j] \overbrace{\sum_{l=1}^{L} \alpha_{kl}^{(1,b)} \int_0^{T_c} \psi(t)\psi\left(t - jT_c - \tau_{kl}^{(1,b)} + 2pT_s - T_s + nT_c\right) \mathrm{d}t}^{f_k^{(1,b)}[n+2pN-N-j]}}_{h_{2,k}^{(1,b)}[p,n]} \\ & + b_{2,k}[i-p] \underbrace{\sum_{j=0}^{N-1} c_{2,k}[j] \overbrace{\sum_{l=1}^{L} \alpha_{kl}^{(2,b)} \int_0^{T_c} \psi(t)\psi\left(t - jT_c - \tau_{kl}^{(2,b)} + 2pT_s + nT_c\right) \mathrm{d}t}^{f_k^{(2,b)}[n+2pN-j]}}_{h_{2,k}^{(2,b)}[p,n]} \\ & + b_{1,k}[i-p] \underbrace{\sum_{j=0}^{N-1} c_{1,k}[j] \overbrace{\sum_{l=1}^{L} \alpha_{kl}^{(2,b)} \int_0^{T_c} \psi(t)\psi\left(t - jT_c - \tau_{kl}^{(2,b)} + 2pT_s - T_s + nT_c\right) \mathrm{d}t}^{f_k^{(2,b)}[n+2pN-N-j]}}_{h_{1,k}^{(2,b)}[p,n]} \Bigg\}. \end{aligned} \tag{134}$$

$$\underline{H}^{(b)}[j] \triangleq \begin{bmatrix} g_{1,1}^{(b)}[j, 0] & \cdots & g_{1,K}^{(b)}[j, 0] & g_{2,1}^{(b)}[j, 0] & \cdots & g_{2,K}^{(b)}[j, 0] \\ \vdots & \vdots & \vdots & \vdots & \vdots & \vdots \\ g_{1,1}^{(b)}[j, 2N-1] & \cdots & g_{1,K}^{(b)}[j, 2N-1] & g_{2,1}^{(b)}[j, 2N-1] & \cdots & g_{2,K}^{(b)}[j, 2N-1] \end{bmatrix}_{2N \times 2K} \tag{138}$$

B. Blind MMSE Space–Time Multiuser Detection

Since the ambient noise is white, i.e., $\mathrm{E}\{\boldsymbol{v}[i]\boldsymbol{v}[i]^H\} = \sigma^2 \boldsymbol{I}_{4Nm}$, the autocorrelation matrix of the received signal in (146) is

$$\boldsymbol{R} \triangleq \mathrm{E}\{\boldsymbol{r}[i]\boldsymbol{r}[i]^H\} = \boldsymbol{H}\boldsymbol{H}^H + \sigma^2 \boldsymbol{I}_{4Nm} \tag{148}$$
$$= \boldsymbol{U}_s \boldsymbol{\Lambda}_s \boldsymbol{U}_s^H + \sigma^2 \boldsymbol{U}_n \boldsymbol{U}_n^H \tag{149}$$

where (149) is the eigendecomposition of $\boldsymbol{R}$. $\boldsymbol{U}_s$ has size $4Nm \times r$, and $\boldsymbol{U}_n$ has size $4Nm \times (4Nm - r)$.

The MMSE space–time multiuser detector and corresponding bit estimate for $b_{a,k}[i]$, $a \in \{1, 2\}$ are given by

$$\boldsymbol{w}_{a,k} \triangleq \arg \min_{\boldsymbol{w} \in \mathcal{C}^{4Pm}} \mathrm{E}\{|b_{a,k}[i] - \boldsymbol{w}^H \boldsymbol{r}[i]|^2\} \tag{150}$$
$$\hat{b}_{a,k}[i] = \mathrm{sign}[\mathrm{Re}\{\boldsymbol{w}_{a,k}^H \boldsymbol{r}[i]\}]. \tag{151}$$

The solution to (150) can be written in terms of the signal subspace components as [26]

$$\boldsymbol{w}_{a,k} = \boldsymbol{U}_s \boldsymbol{\Lambda}_s^{-1} \boldsymbol{U}_s^H \boldsymbol{h}_{a,k} \tag{152}$$

where $\boldsymbol{h}_{a,k} \triangleq \boldsymbol{H}\boldsymbol{e}_{K(2\lceil \iota/2 \rceil + a - 1) + k}$ is the composite signature waveform of user k for bit $a \in \{1, 2\}$. This detector is termed *blind* since it requires knowledge only of the signature sequence of the user of interest. Of course, we also require estimates of the signal subspace components and of the channel. We address the issue of channel estimation next.

C. Blind Adaptive Channel Estimation

In this section, we extend the blind adaptive channel estimation technique described in Section III-B to the asynchronous multipath case. First, however, we describe the discrete-time channel model in order to formulate an analog to the optimization problem in (102).

1) Discrete-Time Channel Model: Using (138) and (143), it is easy to see that

$$\boldsymbol{h}_{a,k} = \begin{bmatrix} g_{a,k}^{(1)}[0,0] \\ \vdots \\ g_{a,k}^{(1)}[0, 2N-1] \\ g_{a,k}^{(2)}[0,0] \\ \vdots \\ g_{a,k}^{(2)}[0, 2N-1] \\ \vdots \\ g_{a,k}^{(1)}[\lceil \iota/2 \rceil, 0] \\ \vdots \\ g_{a,k}^{(1)}[\lceil \iota/2 \rceil, 2N-1] \\ g_{a,k}^{(2)}[\lceil \iota/2 \rceil, 0] \\ \vdots \\ g_{a,k}^{(2)}[\lceil \iota/2 \rceil, 2N-1] \end{bmatrix}_{4N(\lceil \iota/2 \rceil + 1) \times 1}. \tag{153}$$

From (135), we have for $j = 0, \ldots, \lceil \iota/2 \rceil$; $n = 0, \ldots, 2N-1$; $b = 1, 2$

$$g_{1,k}^{(b)}[j,n] = h_{1,k}^{(1,b)}[j,n] + h_{1,k}^{(2,b)}[j,n] \tag{154}$$
$$g_{2,k}^{(b)}[j,n] = h_{2,k}^{(2,b)}[j,n] - h_{2,k}^{(1,b)}[j,n]. \tag{155}$$

We will develop the discrete-time channel model for $g_{1,k}^b[j,n]$. The development for $g_{2,k}^b[j,n]$ follows similarly. From (134), we see that

$$g_{1,k}^b[j,n] = \sum_{q=0}^{N-1} c_{1,k}[q] f_k^{(1,b)}[n + 2jN - q] + \sum_{q=0}^{N-1} c_{1,k}[q] f_k^{(2,b)}[n + 2jN - N - q]. \tag{156}$$

From (134), we can also see that the sequences $f_k^{1,b}[i]$ and $f_k^{2,b}[i]$ are zero whenever $i < 0$ or $i > \iota N$. With this in mind, we define the following vectors:

$$\boldsymbol{g}_{1,k}^{(b)} \triangleq \left[g_{1,k}^{(b)}[0,0] \cdots g_{1,k}^{(b)}[0, 2N-1] \cdots g_{1,k}^{(b)}[\lceil \iota/2 \rceil, 0] \cdots g_{1,k}^{(b)}[\lceil \iota/2 \rceil, 2N-1] \right]^T \tag{157}$$

$$\boldsymbol{f}_{1,k}^{(1,b)} \triangleq \left[f_k^{(1,b)}[0] \cdots f_k^{(1,b)}[\iota N] \underbrace{0 \cdots 0}_{N \text{zeros}} \right]^T \tag{158}$$

$$\boldsymbol{f}_{1,k}^{(2,b)} \triangleq \left[\underbrace{0 \cdots 0}_{N \text{zeros}} f_k^{(2,b)}[0] \cdots f_k^{(2,b)}[\iota N] \right]^T. \tag{159}$$

Then, (157) can be written as

$$\boldsymbol{g}_{1,k}^{(b)} = \boldsymbol{C}_{1,k} \cdot \underbrace{\left[\boldsymbol{f}_{1,k}^{(1,b)} + \boldsymbol{f}_{1,k}^{(2,b)} \right]}_{\boldsymbol{f}_{1,k}^{(b)}} \tag{160}$$

where we have (161), shown at the bottom of the next page.

A similar development for $g_{2,k}^b[j,n]$ produces the result

$$\boldsymbol{g}_{2,k}^{(b)} = \boldsymbol{C}_{2,k} \cdot \underbrace{\left[\boldsymbol{f}_{2,k}^{(2,b)} - \boldsymbol{f}_{2,k}^{(1,b)} \right]}_{\boldsymbol{f}_{2,k}^{(b)}} \tag{162}$$

where

$$\boldsymbol{f}_{2,k}^{(2,b)} \triangleq \left[f_k^{(2,b)}[0] \cdots f_k^{(2,b)}[\iota N] \underbrace{0 \cdots 0}_{N \text{zeros}} \right]^T \tag{163}$$

$$\boldsymbol{f}_{2,k}^{(1,b)} \triangleq \left[\underbrace{0 \cdots 0}_{N \text{zeros}} f_k^{(1,b)}[0] \cdots f_k^{(1,b)}[\iota N] \right]^T. \tag{164}$$

The final task in the section is to form expressions for the composite signature waveforms $\boldsymbol{h}_{1,k}$ and $\boldsymbol{h}_{2,k}$ in terms of the signature matrices $\boldsymbol{C}_{1,k}$, $\boldsymbol{C}_{2,k}$ and the channel response vectors $\boldsymbol{f}_{1,k}^{(b)}$ and $\boldsymbol{f}_{2,k}^{(b)}$. Denote by $\boldsymbol{C}_{a,k}[j]$, $j = 0, 1, \ldots, \lceil \iota/2 \rceil$,

$a \in \{1, 2\}$ the submatrix of $\boldsymbol{C}_{a,k}$ consisting of rows $2Nj+1$ through $2(j+1)N$. Then, it is easy to show that

$$\boldsymbol{h}_{a,k} = \overline{\boldsymbol{C}}_{a,k}\boldsymbol{f}_{a,k} \tag{165}$$

where

$$\overline{\boldsymbol{C}}_{a,k} \triangleq \begin{bmatrix} \boldsymbol{C}_{a,k}[0] & \boldsymbol{0} \\ \boldsymbol{0} & \boldsymbol{C}_{a,k}[0] \\ \boldsymbol{C}_{a,k}[1] & \boldsymbol{0} \\ \boldsymbol{0} & \boldsymbol{C}_{a,k}[1] \\ \vdots & \vdots \\ \boldsymbol{C}_{a,k}[\lceil \iota/2 \rceil] & \boldsymbol{0} \\ \boldsymbol{0} & \boldsymbol{C}_{a,k}[\lceil \iota/2 \rceil] \end{bmatrix}_{4N(\lceil \iota/2 \rceil+1)\times(2N(\iota+1)+2)}$$

and

$$\boldsymbol{f}_{a,k} \triangleq \begin{bmatrix} \boldsymbol{f}_{a,k}^{(1)} \\ \boldsymbol{f}_{a,k}^{(2)} \end{bmatrix}_{(2N(\iota+1)+2)\times 1}. \tag{166}$$

2) Blind Sequential Kalman Channel Estimation: The blind channel estimation problem for the asynchronous multipath case involves the estimation of $\boldsymbol{f}_{a,k}(1 \le k \le K,\ a = 1, 2)$ from the received signal $\boldsymbol{r}[i]$. As we did for the synchronous case, we will exploit the orthogonality between the signal subspace and noise subspace. Specifically, since $\boldsymbol{U}_n$ is orthogonal to the columnspace of $\boldsymbol{H}$, we have

$$\boldsymbol{U}_n^H \boldsymbol{h}_{a,k} = \boldsymbol{U}_n^H \overline{\boldsymbol{C}}_{a,k}\boldsymbol{f}_{a,k} = \boldsymbol{0}. \tag{167}$$

Denote by $\boldsymbol{z}[i]$ the projection of the received signal $\boldsymbol{r}[i]$ onto the noise subspace, i.e.,

$$\begin{aligned} \boldsymbol{z}[i] &= \boldsymbol{r}[i] - \boldsymbol{U}_s\boldsymbol{U}_s^H\boldsymbol{r}[i] & (168)\\ &= \boldsymbol{U}_n\boldsymbol{U}_n^H\boldsymbol{r}[i]. & (169)\end{aligned}$$

Using (167), we have

$$\boldsymbol{f}_{a,k}^H \overline{\boldsymbol{C}}_{a,k}^H \boldsymbol{z}[i] = 0. \tag{170}$$

Our channel estimation problem, then, involves the solution of the optimization problem

$$\hat{\boldsymbol{f}}_{a,k} = \arg\min_{\boldsymbol{f}} E\left\{ \left| \boldsymbol{f}^H \overline{\boldsymbol{C}}_{a,k}^H \boldsymbol{z}[i] \right|^2 \right\} \tag{171}$$

subject to the constraint $\|\boldsymbol{f}\| = 1$. If we denote $\boldsymbol{x}[i] \triangleq \overline{\boldsymbol{C}}_{a,k}^H \boldsymbol{z}[i]$, then we can use the Kalman-type algorithm described in (103)–(105), where $\boldsymbol{h}_1[i]$ is replaced with $\boldsymbol{f}_{a,k}[i]$.

Note that a necessary condition for the channel estimate to be unique is that the matrix $\boldsymbol{U}_n^H \overline{\boldsymbol{C}}_{a,k}$ is tall, i.e., $4Nm - 2K(m + \lceil \iota/2 \rceil) \ge 2N(\iota+1)+2$. Therefore, we choose the smoothing factor m such that

$$m \ge \left\lceil \frac{N(\iota+1) + K\lceil \iota/2 \rceil + 1}{2N - K} \right\rceil. \tag{172}$$

Using the same constraint, we find that for a fixed m, the maximum number of users that can be supported is

$$\min\left\{ \left\lfloor \frac{N(2m - \iota - 1) - 1}{m + \lceil \iota/2 \rceil} \right\rfloor, \left\lfloor \frac{N}{2} \right\rfloor \right\}. \tag{173}$$

Notice that for reasonable choices of m and ι, (173) is larger than the maximum number of users for the linear diversity receiver structure, which is given by

$$\left\lfloor \frac{N(m-\iota)}{2(m+\iota)} \right\rfloor. \tag{174}$$

This represents a quantitative example of the capacity benefit of space–time multiuser detection discussed in Section II-D.

Once an estimate of the channel state $\hat{\boldsymbol{f}}_{a,k}$ is obtained, the composite signature vector of the kth user for bit a is given by (165). Note that there is an arbitrary phase ambiguity in the estimated channel state, which necessitates differential encoding and decoding of the transmitted data.

D. Algorithm Summary

Algorithm 3 [Blind Adaptive Linear Space–Time Multiuser Detector—Asynchronous Multipath CDMA, Two Transmitter Antennas and Two Receiver Antennas]:

- Stack matched filter outputs in (131) according to (139), (141), and (144) to create $\boldsymbol{r}[i]$.
- Create $\overline{\boldsymbol{C}}_{a,k}$ according to (166).

$$\boldsymbol{C}_{1,k} \triangleq \begin{bmatrix} c_{1,k}[0] & & \\ c_{1,k}[1] & \ddots & \\ \vdots & \ddots & c_{1,k}[0] \\ \vdots & & c_{1,k}[1] \\ c_{1,k}[N-1] & & \vdots \\ & \ddots & \vdots \\ & & c_{1,k}[N-1] \end{bmatrix}_{(2N(\lceil \iota/2 \rceil+1))\times(N(\iota+1)+1)} \tag{161}$$

- Using a suitable signal subspace tracking algorithm, e.g., NAHJ-FST, update the signal subspace components $\boldsymbol{U}_s[i]$ and $\boldsymbol{\Lambda}_s[i]$ at each time slot i.
- Track the channel $\boldsymbol{f}_{a,k}$ $(1 \le k \le K,\ a = 1, 2)$ according to

$$\boldsymbol{z}[i] = \boldsymbol{r}[i] - \boldsymbol{U}_s[i]\boldsymbol{U}_s[i]^H\boldsymbol{r}[i] \tag{175}$$

$$\boldsymbol{x}[i] = \overline{\boldsymbol{C}}_{a,k}^H\boldsymbol{z}[i] \tag{176}$$

$$\boldsymbol{k}[i] = \boldsymbol{\Sigma}[i-1]\boldsymbol{x}[i](\boldsymbol{x}[i]^H\boldsymbol{\Sigma}[i-1]\boldsymbol{x}[i])^{-1} \tag{177}$$

$$\boldsymbol{f}_{a,k}[i] = \boldsymbol{f}_{a,k}[i-1] - \boldsymbol{k}[i](\boldsymbol{x}[i]^H\boldsymbol{f}_{a,k}[i-1]) \Big/ \|\boldsymbol{f}_{a,k}[i-1] - \boldsymbol{k}[i](\boldsymbol{x}[i]^H\boldsymbol{f}_{a,k}[i-1])\| \tag{178}$$

$$\boldsymbol{\Sigma}[i] = \boldsymbol{\Sigma}[i-1] - \boldsymbol{k}[i]\boldsymbol{x}[i]^H\boldsymbol{\Sigma}[i-1]. \tag{179}$$

- Form the detectors

$$\boldsymbol{w}_{a,k}[i] = \boldsymbol{U}_s[i]\boldsymbol{\Lambda}_s^{-1}[i]\boldsymbol{U}_s[i]^H\overline{\boldsymbol{C}}_{a,k}\boldsymbol{f}_{a,k}[i]. \tag{180}$$

- Perform differential detection

$$z_{a,k}[i] = \boldsymbol{w}_{a,k}[i]^H\boldsymbol{r}[i], \tag{181}$$

$$\hat{\beta}_{a,k}[i] = \text{sign}(\Re\{z_{a,k}[i]\ z_{a,k}[i-1]^*\}). \tag{182}$$

V. Simulation Results

In this section, we present simulation results to illustrate the performance of blind adaptive space–time multiuser detection. We first look at the synchronous flat-fading case; then, we consider the asynchronous multipath-fading scenario. For all simulations, we use the two transmit/two receive antenna configuration. The m-sequences of length 15 and their shifted versions are employed as user spreading sequences. The chip pulse is a raised cosine with roll-off factor 0.5. For the multipath case, each user has $L = 3$ paths. The delay of each path is uniform on $[0, T_s]$. Hence, the maximum delay spread is one symbol interval, i.e., $\iota = 1$. The fading gain for each users' channel is generated from a complex Gaussian distribution and is fixed for all simulations. The path gains in each users's channel are normalized so that each users's signal arrives at the receiver with the same power. The smoothing factor is $m = 2$, and the forgetting factor for the subspace tracking algorithm for all simulations is 0.995. The performance measures are bit-error probability and signal-to-interference-plus-noise ratio, which are defined by SINR $\triangleq E^2\{\boldsymbol{w}^H\boldsymbol{r}\}/\text{Var}\{\boldsymbol{w}^H\boldsymbol{r}\}$, where the expectation is with respect to the data bits of interfering users and the ambient noise. In the simulations, the expectation operation is replaced by the time averaging operation. SINR is a particularly appropriate figure of merit for MMSE detectors since it has been shown [27] that the output of an MMSE detector is approximately Gaussian distributed. Hence, the SINR values translate directly and simply to bit-error probabilities, i.e., $\Pr(e) \approx Q(\sqrt{\text{SINR}})$. The labeled horizontal lines on the SINR plot represent bit-error-probability thresholds. For the SINR plots, the number of users for the first 1500 iterations is 4. At iteration 1501, three users are added so that the system is fully loaded. At iteration 3001, five users are removed. For the BER plots, the frame size is 200 bits, and the system is allowed 1000 bits to reach steady state before errors are accumulated.

Fig. 2 illustrates the adaptation performance for the synchronous, flat-fading case. The SNR is fixed at 8 dB. Notice that the bit-error probability does not drop below 10^{-3}, even during transitions when users enter or leave the system.

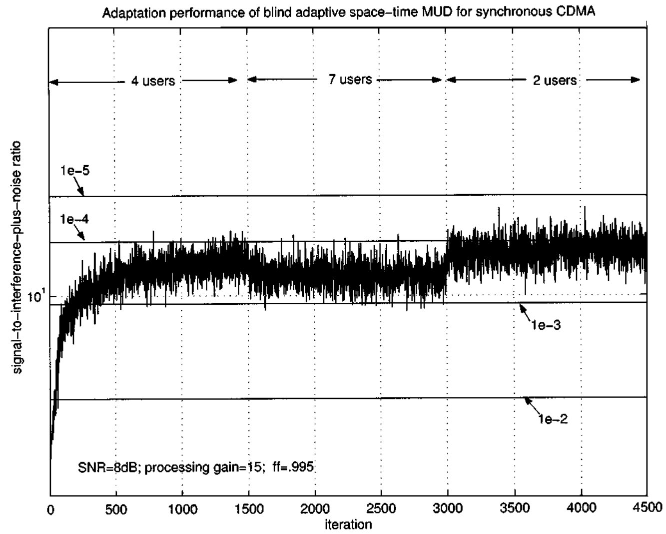

Fig. 2. Adaptation performance of space–time multiuser detection for synchronous CDMA. The labeled horizontal lines represent bit-error-probability thresholds.

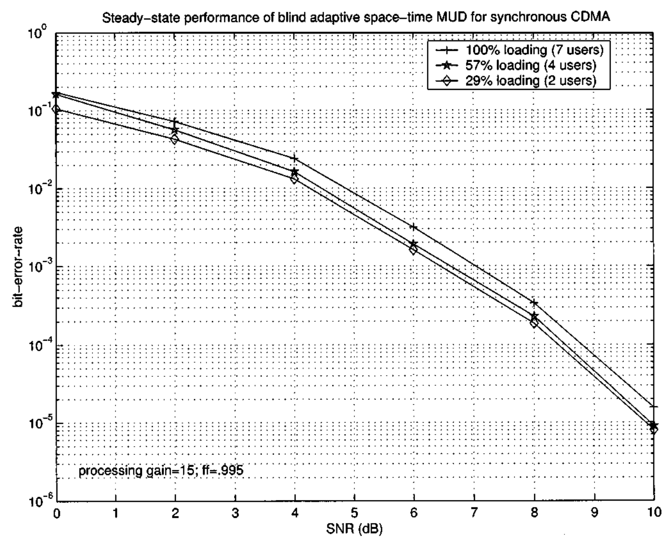

Fig. 3. Steady-state performance of space–time multiuser detection for synchronous CDMA.

Fig. 3 shows the steady-state performance for the synchronous case for different system loads. We see that the performance changes little as the system load changes. Although an error floor is unavoidable since we are estimating the detectors and the channel from the received signal, it is sufficiently low so that it does not appear in this figure.

Fig. 4 shows the adaptation performance for the asynchronous multipath case. The SNR for this simulation is 11 dB. Again, notice that the bit-error-probability does not drop significantly as users enter and leave the system.

Fig. 5 shows the steady-state performance for the asynchronous multipath case for different system loads. It is seen that system loading has a more significant effect on performance for the asynchronous multipath case that it does for the synchronous case.

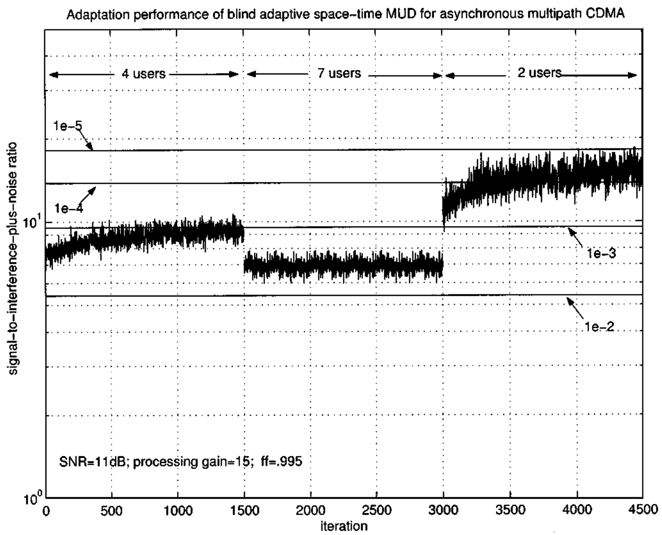

Fig. 4. Adaptation performance of space–time multiuser detection for asynchronous multipath CDMA. The labeled horizontal lines represent bit-error-probability thresholds.

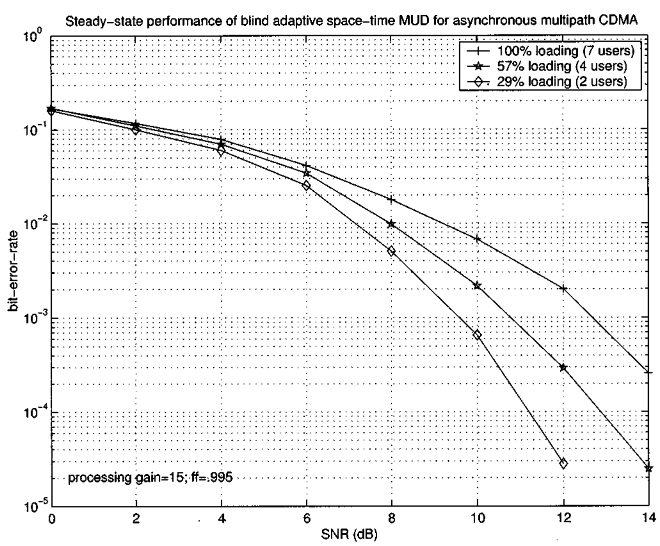

Fig. 5. Steady-state performance of space–time multiuser detection for asynchronous multipath CDMA.

VI. Conclusion

In this work, we have analyzed and compared two different linear receiver structures that are appropriate for CDMA systems with multiple transmit and receive antennas. We have seen that the space–time structure has many advantages over linear diversity combining, including better bit-error-rate performance (for configurations with 1 transmit antenna and 2 or more receive antennas), lower complexity, and higher user capacity. We have also developed blind adaptive implementations of the space–time structure for synchronous CDMA channels in flat-fading channels and for asynchronous CDMA in fading multipath channels. Finally, we have presented simulations to illustrate the steady-state and adaptation performance of the adaptive receiver.

References

[1] T. Ojanperä and R. Prasad, *Wideband CDMA for Third Generation Mobile Communications*. Norwood, MA: Artech House, 1998.

[2] X. Wang and H. V. Poor, "Space–time multiuser detection in multipath CDMA channels," *IEEE Trans. Signal Processing*, vol. 47, pp. 2356–2374, Sept. 1999.

[3] T. F. Wong, T. M. Lok, J. S. Lehnert, and M. D. Zoltowski, "A linear receiver for direct-sequence spread-spectrum multiple-access with antenna array and blind adaptation," *IEEE Trans. Inform. Theory*, vol. 44, pp. 659–677, Mar. 1998.

[4] H. Liu and M. D. Zoltowski, "Blind equalization in antenna array CDMA systems," *IEEE Trans. Signal Processing*, vol. 45, pp. 161–172, Jan. 1997.

[5] A. J. Paulraj and C. B. Papadias, "Space–time processing for wirless communications," *IEEE Signal Processing Mag.*, vol. 14, pp. 49–83, Nov. 1997.

[6] X. Bernstein and A. M. Haimovic, "Space–time processing for increased capacity of wireless CDMA," in *Proc. ICC*, 1996, pp. 597–601.

[7] S. Miller and S. C. Schwartz, "Integrated spatial–temporal detectors for asynchronous Gaussian multiple access channels," *IEEE Trans. Commun.*, vol. 43, pp. 396–411, Feb./Mar./Apr. 1995.

[8] B. Suard *et al.*, "Performance of CDMA mobile communications systems using antenna arrays," in *Proc. ICASSP*, 1993.

[9] A. Wittneben, "Base station modulation diversity for digital SIMULCAST," in *Proc. IEEE Veh. Technol. Conf.*, 1993, pp. 505–511.

[10] ——, "A new bandwidth efficient transmit antenna modulation diversity scheme for linear digital modulation," in *Proc. Int. Conf. Commun.*, 1993, pp. 1630–1634.

[11] N. Seshadri and J. H. Winters, "Two signaling schemes for improving the error performance of frequency-division duplex (FDD) transmission systems using transmitter antenna diversity," in *Proc. IEEE Veh. Technol. Conf.*, May 1993, pp. 508–511.

[12] J. H. Winters, "The diversity gain of transmit diversity in wireless systems with Rayleigh fading," in *Proc. ICC/SUPERCOMM*, vol. 2, New Orleans, LA, May 1994, pp. 1121–1125.

[13] V. Tarokh, N. Seshadri, and A. R. Calderbank, "Space–time codes for high data rate wireless communications: Performance criterion and code construction," *IEEE Trans. Inform. Theory*, vol. 44, pp. 744–765, Mar. 1998.

[14] S. Alamouti, "A simple transmit diversity technique for wireless communications," *IEEE J. Select. Areas Commun.*, vol. 16, pp. 1451–1458, Oct. 1998.

[15] Texas Instruments Inc., "Space–time block coded transmit antenna diversity for WCDMA,", proposed TDOC#662/98 to ETSI SMG2 UMTS stand., Dec. 1998.

[16] Lucent Technol., "Downlink diversity improvements through space–time spreading,", proposed 3GPP2-C30-19 990 817-014 to the CDMA-2000 stand., Aug. 1999.

[17] V. Tarokh, H. Jafarkhani, and A. R. Calderbank, "Space–time block codes from orthogonal designs," *IEEE Trans. Inform. Theory*, vol. 45, pp. 1456–1467, July 1999.

[18] G. J. Forschini and M. J. Gans, "On limits of wireless communications in a fading environment when using multiple antennas," *Wireless Pers. Commun.*, vol. 6, no. 3, pp. 311–335, 1998.

[19] I. Telatar, "Capacity of multi-antenna Gaussian channels," *Eur. Trans. Telecommun.*, vol. 10, pp. 585–595, Nov.–Dec. 1999.

[20] H. Huang and H. Viswanathan, "Multiple antennas and multiuser detection in high data rate CDMA systems," in *Proc. IEEE Veh. Technol. Conf.*, Tokyo, Japan, 2000, pp. 556–560.

[21] B. Hochwald, T. L. Marzetta, and C. B. Papadias, "A transmitter diversity scheme for wideband CDMA systems based on space–time spreading," *IEEE J. Select. Areas Commun.*, vol. 19, pp. 48–60, Jan. 2001.

[22] S. Verdú, *Multiuser Detection*. Cambridge, U.K.: Cambridge Univ. Press, 1998.

[23] X. Wang and H. V. Poor, "Blind multiuser detection: A subspace approach," *IEEE Trans. Inform. Theory*, vol. 44, pp. 677–691, Mar. 1998.

[24] X. Wang and A. Høst-Madsen, "Group-blind multiuser detection for uplink CDMA," *IEEE J. Select. Areas Commun.*, vol. 17, pp. 1971–1984, Nov. 1999.

[25] D. Reynolds and X. Wang, "Adaptive group-blind multiuser detection based on a new subspace tracking algorithm," *IEEE Trans. Commun.*, vol. 49, pp. 1135–1141, July 2001.

[26] X. Wang and H. V. Poor, "Blind equalization and multiuser detection for CDMA communications in dispersive channels," *IEEE Trans. Commun.*, vol. 46, pp. 91–103, Jan. 1998.

[27] H. V. Poor and S. Verdú, "Probability of error in MMSE multiuser detection," *IEEE Trans. Inform. Theory*, vol. 43, pp. 858–871, May 1997.

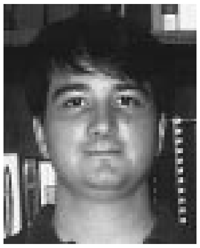

Daryl Reynolds received the B.S. degree in electrical engineering from the University of Colorado, Boulder, in 1993 and the M.S. degree in electrical engineering from Texas A&M University, College Station, in 1998. He is currently pursuing the Ph.D. degree with the Department of Electrical Engineering, Texas A&M University.

Since 1996, he has been an Assistant Lecturer and Teaching Assistant with this department. His research interests include multiuser communication theory and statistical signal processing for wireless communications.

Xiaodong Wang (M'98) received the B.S. degree in electrical engineering and applied mathematics (with the highest honor) from Shanghai Jiao Tong University, Shanghai, China, in 1992, the M.S. degree in electrical and computer engineering from Purdue University, West Lafayette, IN, in 1995, and the Ph.D. degree in electrical engineering from Princeton University, Princeton, NJ, in 1998.

From July 1998 to December 2001, he was an Assistant Professor with the Department of Electrical Engineering, Texas A&M University, College Station. In January 2002, he joined the Department of Electrical Engineering, Columbia University, New York, NY, as an Assistant Professor. His research interests fall in the general areas of computing, signal processing, and communications. He has done work in the areas of digital communications, digital signal processing, parallel and distributed computing, nanoelectronics and quantum computing, and he has published extensively in these areas. His current research interests include multiuser communications theory and advanced signal processing for wireless communications. He was with AT&T Labs—Research, Red Bank, NJ, during the summer of 1997.

Dr. Wang received the 1999 NSF CAREER Award and the 2001 IEEE Communications Society and Information Theory Society Joint Paper Award. He currently serves as an Associate Editor for the IEEE TRANSACTIONS ON COMMUNICATIOINS, the IEEE TRANSACTIONS ON SIGNAL PROCESSING, and the IEEE TRANSACTIONS ON WIRELESS COMMUNICATIONS.

H. Vincent Poor (S'72–M'77–SM'82–F'87) received the Ph.D. degree in electrical engineering and computer science in 1977 from Princeton University, Princeton, NJ.

He is currently a Professor of electrical engineering at Princeton. He is also affiliated with Princeton's Department of Operations Research and Financial Engineering and with its Program in Applied and Computational Mathematics. From 1977 until he joined the Princeton faculty in 1990, he was a Faculty Member at the University of Illinois at Urbana-Champaign. He has also held visiting and summer appointments at several universities and research organizations in the United States, Britain, and Australia. His research interests are primarily in the area of statistical signal processing, with applications in wireless communications and related areas. Among his publications in this area is the book *Wireless Communications: Signal Processing Perspectives*.

Dr. Poor is a member of the National Academy of Engineering and is a Fellow of the Acoustical Society of America, the American Association for the Advancement of Science, the Institute of Mathematical Statistics, and the Optical Society of America. His IEEE activities include serving as the President of the IEEE Information Theory Society in 1990 and as a member of the IEEE Board of Directors from 1991 to 1992. Among his honors are the Frederick E. Terman Award of the American Society for Engineering Education (1992), the Distinguished Member Award from the IEEE Control Systems Society (1994), an IEEE Third Millennium Medal (2000), the IEEE Graduate Teaching Award (2001), and the first Joint Paper Award of the IEEE Communications Society and IEEE Information Theory Society (2002).